Physics

NOV 8 1961

COLE MEMORIAL LIBRARY

SCIENCE OF LIGHT

VOLUME 9 NUMBER 3

December
1960

OHIO STATE UNIVERSITY
NOV 6 - 1961
LIBRARY

Published by the

Institute for Optical Research

Tokyo University of Education

in collaboration with

The Spectroscopical Society of Japan

SCIENCE OF LIGHT

Science of Light contains reports of the Institute for Optical Research and contribution from other science bodies about similar subjects

The editorial staff consists of following members:

Chairman: Prof. H. Ootsuka, *Tokyo University of Education*

Dr. Y. Fujioka, *Saitama University*

Prof. E. Minami, *Tokyo University*

Prof. M. Seya, *Tokyo University of Education*

Prof. Y. Uchida, *Kyoto University*

Prof. T. Uemura, *Rikkyo University*

Prof. K. Miyake, *Tokyo University of Education*

All communications should be addressed to the director or to the librarian of the Institute.

The Institute for Optical Research

Tokyo University of Education

400, Hyakunin-tyo-4, Shinzyuku-ku, Tokyo, Japan

Printed by
Kabushiki Kaisha Kokusai Insatsu,
Tokyo

Preparation of Uniform Layer of Sodium Salicylate

Fumio MASUDA

Urawa the First Girl's High School, Urawa Japan

Masao SEYA

Institute for Optical Research, Tokyo University of Education
Shinzyuku-ku Tokyo

(Received December 30, 1960)

Abstract

Methods for preparing uniform layer of sodium salicylate are described. The layer most suited for detection of extreme ultraviolet is of approximately one milligram of sodium salicylate per square centimeter.

1. Introduction

The intensity of extreme ultraviolet is usually measured by the intensity of fluorescent light emitted by some material under illumination of the rays. As the fluorescent material in most cases, sodium salicylate is being used, which is made into a layer on glass or on outside of photomultiplier tube, and the transmitted light is measured photoelectrically. No work has so far been known as to the method of preparing uniform layer of sodium salicylate and the suitable thickness of the layer, which made the authors go further into the matter by experimentation.

2. Preparation of uniform layer of sodium salicylate

Ordinary method of obtaining sodium salicylate layer is to spread saturated solution of sodium salicylate in methyl alcohol on surface of glass or directly on photomultiplier tube and evaporate the solvent. With this method, however, uneven formation of small crystals during drying gives difficulty in obtaining uniformity of the layer. Among several methods that were tried, the following were found feasible.

Method I. Use of saturated solution of sodium salicylate in a mixture of methyl alcohol and methyl ethyl ketone

The solvent is a mixture of equal amounts of methyl alcohol and methyl ethyl

ketone. On a piece of glass plate, saturated solution of sodium salicylate is let out of an injection needle laid flat and moved sideways on the surface. This gives even spread of the solution which, when dried in oven at 80°C, becomes a layer of uniform thickness.

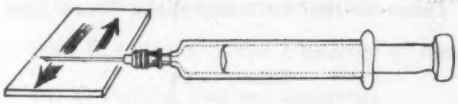

Fig. 1.

Method II. Dipping of a piece of glass plate into hot and saturated ethyl alcohol solution

A piece of glass plate is dipped into saturated solution of sodium salicylate in ethyl alcohol at a temperature a few degree below boiling point for 2~3 seconds and dried on electric heater. Repetition of this process gives a uniform layer of desired thickness. This method is useful for obtaining thick uniform layers. Table 1 shows

Table 1.

Number of repetition of the process	1	2	3	4	5	6	7	8	9	10	11
Quantity of sodium salycilate (mg)	0.4	0.6	1.1	1.7	1.8	3.2	4.4	4.8	6.2	9.3	10.7

the relation between the quantity of sodium salicylate per cm^2 and the number of repetition of the process, the size of the glass plate being 24×28×1.2 mm. In this method, grain size increases as the temperature of the solution is lowered.

Method III. From suspension of sodium salicylate in isoamyl alcohol

Sodium salicylate is mixed with isoamyl alcohol (dispersive medium) and ground

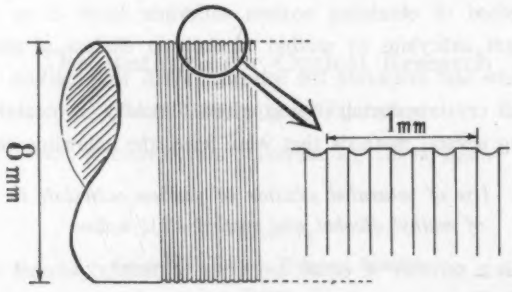

Fig. 2.

in a ceramic mortar. By this method, fine grain suspension is obtained which can be preserved for several months. The suspension is spread over a piece of glass plate with a draw down rod used by paint manufacturers which has fine spiral grooves on its surface as shown in Fig. 2. Gentle smoothing by this rod gives even spread of the suspension, which is dried in oven at 90°C for about 10 minutes to complete the la yer.

Method IV. By spraying

Saturated solution of sodium salicylate in ethyl alcohol is sprayed on a piece of glass plate laid on a hot metal plate. Fig. 3 shows the apparatus used for this method.

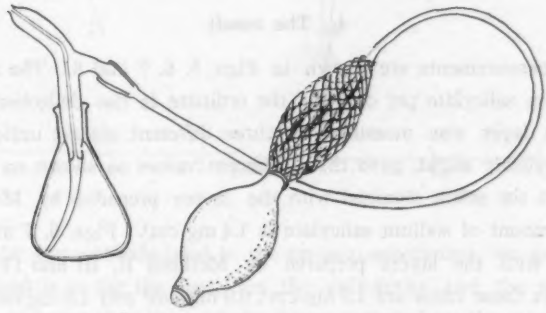

Fig. 3.

3. Efficiency of sodium salicylate layer

2537 A mercury line as the excitation source of light, experiments were made on the efficiency of the layer in extreme ultraviolet detection. Since sodium salycilate layer has a constant quantum efficiency over a wide wavelength range, a layer of

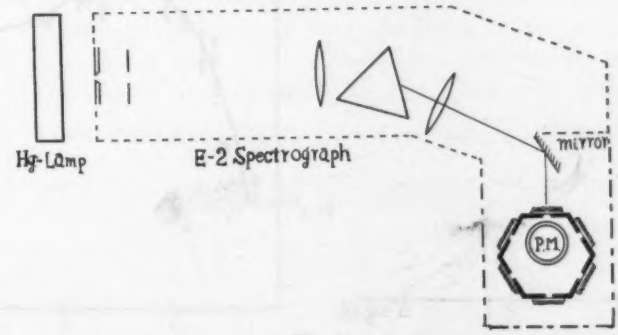

Fig. 4.

certain thickness which has good sensitivity for 2537 A will be equally sensitive to extreme ultraviolet.

The apparatus used in this experiment is shown in Fig. 4. The light source is a quartz mercury lamp and the monochromator is a Hilger E-2 type spectrograph. The photomultiplier tube is covered with a hexagonal case which is made to be turned by hand. Every face of the case has a window fitted with a glass plate; each plate has a sodium salicylate layer of different thickness so that, by turning the case, relative values of efficiency of these six layers can be measured. The distance between the photomultiplier tube and the layer in measuring position is about 1.5 cm.

4. The result

Results of measurements are shown in Figs. 5, 6, 7 and 8. The abscissa is the amount of sodium salicylate per cm^2 and the ordinate is the deflection of a micro-ammeter. Each layer was measured at three different places; uniformness of the layer, though invisibly slight, gave three different values as shown on the figures.

Fig. 5 shows the result obtained with the layers prepared by Method I. The most suitable amount of sodium salicylate is 1.4 mg/cm^2. Figs. 6, 7 and 8 show the results obtained with the layers prepared by Methods II, III and IV and the most suitable values in these cases are 1.5 mg/cm^2, 0.9 mg/cm^2 and 1.0 mg/cm^2 respectively. The difference in the suitable values for layers prepared by different methods seems attributable to the difference in grain size of sodium salicylate.

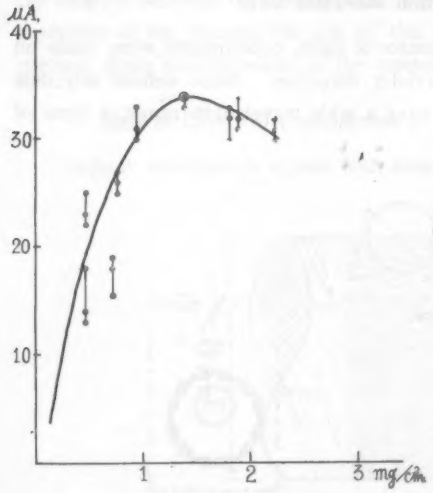

Fig. 5.

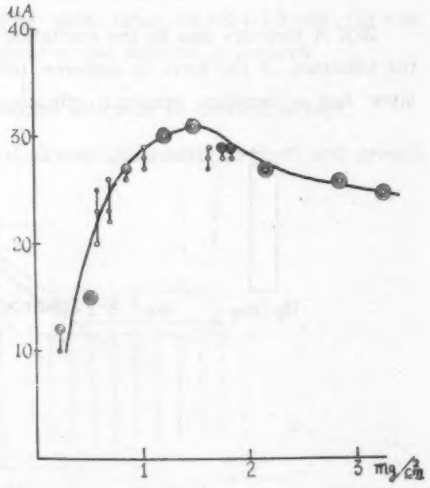

Fig. 6.

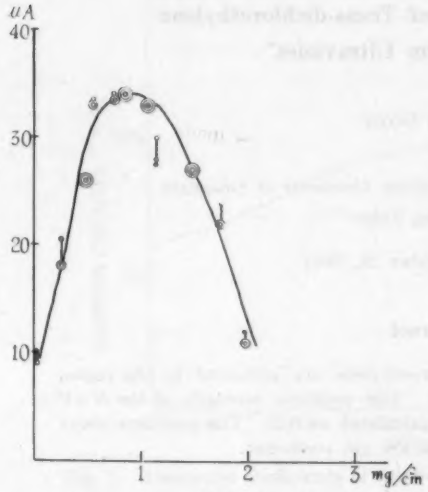

Fig. 7.

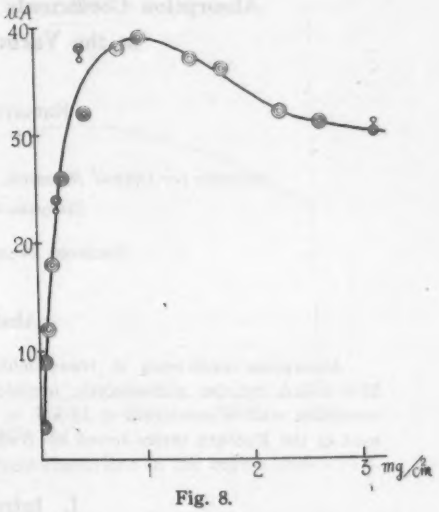

Fig. 8.

Measured by the methods tried in the present experiment, we may conclude that the spray method is so far the best, for the uniformity and the sensitivity of the layer appear to be better than those of the layers prepared by the other three methods as can be seen on the figures. Considering that the form of all the curves is asymmetric with respect to the efficiency, we should for safety better prepare the layer somewhat thicker than what the peak of the curve signifies.

Absorption Coefficients of Trans-dichlorethylene in the Vacuum Ultraviolet*

Katsuya GOTO

Institute for Optical Research, Tokyo University of Education
Sinzyuku-ku, Tokyo

(Recieved December 30, 1960)

Abstract

Absorption coefficients of trans-dichloroethylene are measured in the region 2100–1050 A by the photoelectric method. The oscillator strength of the $N \rightarrow V$ transition with a maximum at 1975 A is calculated as 0.22. The members above $n=4$ of the Rydberg series found by Walsh are not confirmed.

1. Introduction

Aosorption spectrum of trans-dichloroethylene in the vacuum ultraviolet has been studied by Mahncke and Noyes[1], and Walsh.[2] The former could not find any Rydberg series and made tentative classifications of discrete bands, and the latter found a Rydberg series converging to 9.91 e. v. and made an analysis which is vibrational, different from the former.

On the other hand, deduced from the result of his work by the photoionization method, Watanabe considered 9.63 e.v. to be the ionization potential.[3]

In the present study, absorption coefficients of this molecule are measured at several hundred points in the region 2100–1050 A by the photoelectric method initiated by Watanabe,[4] and from these data, establishments of the ionization potential and the vibrational assignment are attempted.

2. Experimental

Measurement of absorption coefficients was made after Watanabe et al's method.

* This experiment was carried out at Department of Physics, University of Hawaii, and sponsored in part by the Geophysics Research Center, ARDC, under contract AF 19 (604)-1390 with University of Hawaii.

1) H. E. Mahncke and W. A. Noyes, Jr.: J. Chem. Phys. **3** (1935) 536.
2) A. D. Walsh: Trans. Faraday Soc. **41** (1945) 35.
3) K. Watanabe: Private communication.
4) K. Watanabe, E. C. Inn, and M. Zelikoff: J. Chem. Phys. **21** (1935) 1026.

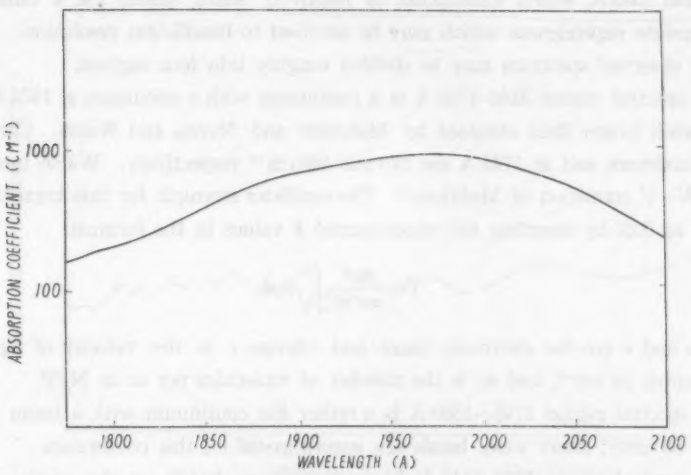

Fig. 1. Absorption coefficients of trans-dichloroethylene in the region 2100–1775 A.

For convenience, the method is outlined below.

The main apparatus consists of a 1 m vacuum monochromator, a hydrogen discharge tube operated at 400 mA and 600 v dc, EMI-9514 B photomultiplier coated with sodium salicylate as detector, and an absorption cell of 10 cm in length with LiF windows. The absorption cell is placed between the exit slit of monochromator and the detector. A grating ruled 1200 lines per mm and slits of 0.01 mm width provide a resolution of about 0.2 A, and the spectrum is scanned at 2.5 A per minute. As the sample, Kodaks' reagent was used.

The absorption coefficient k in cm^{-1} is defined by the equation $I=I_0 \exp(-kx)$, where I_0 and I are the incident and transmitted light intensities and x is the NTP-reduced layer thickness in cm of the absorping gas. Measurements were made under a number of pressures, ranging from 1.6 to 0.04 mmHg, at 25°C. Pressures below 0.5 mmHg were measured with a Consolidated micromanometer, type 23-105. From recorder tracings obtained with different pressures, four or six k values were computed at each of about 420 wavelengths.

3. Results and Discussion

Mean absorption coefficients of trans-dichloroethylene in the spectral region from 1075 A to 2100 A are summarized in Figs. 1~5, which were made by drawing smooth curves through points for about 420 wavelengths. Experimental error in estimating the mean k value is about 5% for nearly all wavelengths. At wavelengths between

1440 A and 1545 A, which correspond to relatively sharp bands, the k values show some pressure dependences which may be ascribed to insufficient resolution.

The observed spectrum may be divided roughly into four regions.

1) The spectral region 2100–1745 A is a continuum with a maximum at 1975 A which is somewhat longer than obtained by Mahncke and Noyes, and Walsh. Coefficients at the maximum and at 1745 A are 970 and 160 cm^{-1} respectively. Walsh interpreted this as $N \rightarrow V$ transition of Mulliken.[5] The oscillator strength for this transition was obtained as 0.22 by inserting the experimental k values in the formula

$$f = \frac{mc^2}{\pi e^2 n_0} \int_{\nu_2}^{\nu_1} k_\nu d_\nu$$

where m and e are the electronic mass and charge, c is the velocity of light, ν is wave number in cm^{-1}, and n_0 is the number of molecules per cc at NTP.

2) The spectral region 1745~1560 A is a rather flat continuum with a mean k value of about 80 cm^{-1}; many weak bands are superimposed on this continuum.

3) The spectral region 1560–1440 A has many sharp bands on the continuum, the intensity of which increases toward the shorter wavelength side. The k values are nearly independent of pressure, but vary considerably with some wavelengths. The smoothing of the absorption curves is done by considering the results of Mahncke and Noyes, and Walsh. As shwon Fig. 3, all bands assigned by Walsh are found, but some of Mahncke and Noyes' are not confirmed.

4) The spectral region below 1440 A has two very strong bands, 1425 A and 1375 A. To these bands Walsh assigned $n=3$ and $n=4$ members of a Rydberg series converging to 9.91 e.v. and found other members up to $n=8$. As shown in Fig. 4, $n=6$ 7 and 8 members seem to be present, but their intensities are much too low. Their k values and their backgound continua are

	Wavelengths (A)	Rydberg bands	Background continua
$n=3$	1425	3200	800
$n=4$	1375	2000	900
$n=5$		—	1100
$n=6$	1290	1400	1300
$n=7$	1278	1450	1400
$n=8$	1270	1700	1550

On the other hand, a Rydberg series converging to 9.63 e.v.——ionization potential by photoionization method——could not be found.

In conclusion, the author wishes to express his sincere gratitude to Dr. Watanabe of University of Hawaii for his encouragement during the course of this work.

5) R. S. Mulliken: J. Chem. Phys. **3** (1935) 514.

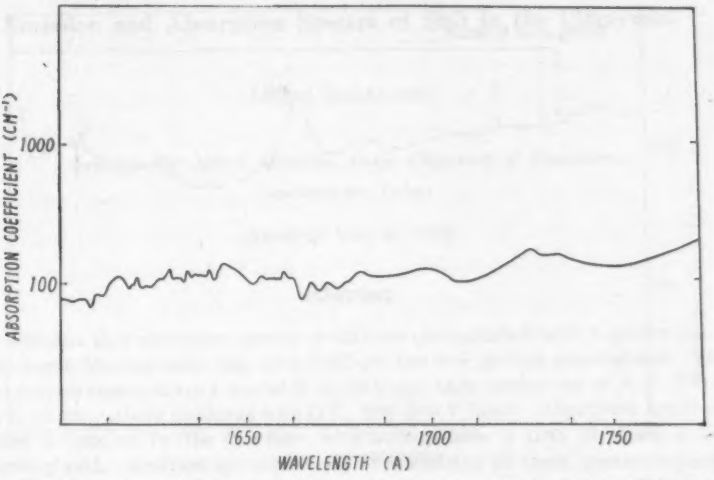

Fig. 2. Absorption coefficients of trans-dichloroethylene in the region 1775–1600 A.

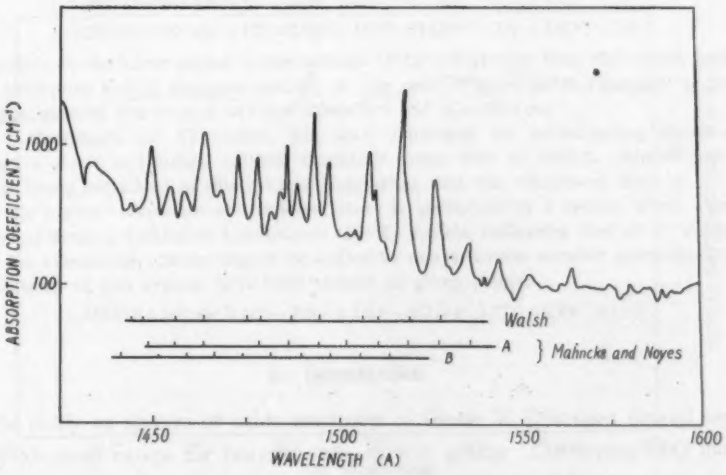

Fig. 3. Absorption coefficients of trans-dichloroethylene in the region 1425–1600 A.

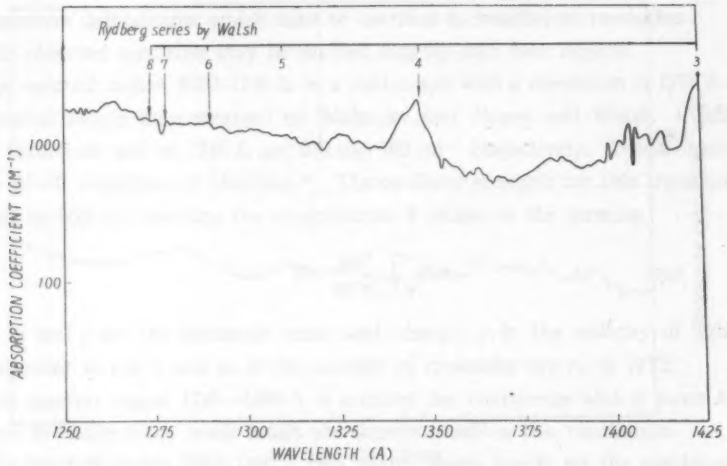

Fig. 4. Absorption coefficients of trans-dichloroethylene in the region 1250–1425 Å.

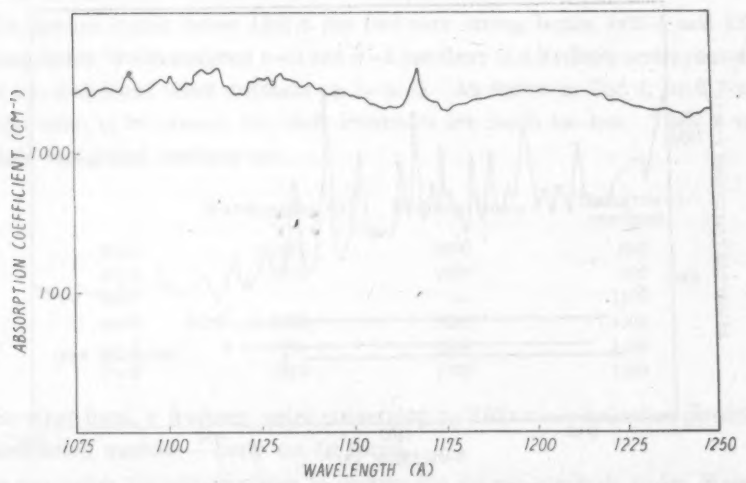

Fig. 5. Absorption coefficients of trans-dichloroethylene in the region 1075–1250 Å.

Emission and Absorption Spectra of SbO in the Ultraviolet

Midori SHIMAUCHI

Institute for Optical Research, Tokyo University of Education
Sinzyuku-ku, Tokyo

(Received Dec. 30, 1960)

Abstract

Emission and absorption spectra of SbO are photographed with a quartz and a glass prism spectrographs, also with a 665 cm concave grating spectrograph. The light sources employed are a special D. C. 100 V arc, high tension arc of A. C. 7500 V and a hollow cathode discharge with D. C. 1000-2000 V input. Absorption spectrum of SbO is observed for the first time with a flame from a D. C. 100 V arc as an absorbing path. Analyses are carried out by comparing all these spectra in region of 4400-2450 A.

Sengupta's ultraviolet system is re-investigated at first with much help of absorption spectrum from 2450 A to 2800 A. Many so called "extra" heads are observed in this system, and on the basis of regularity in the difference of heads, a new analysis has been made. Q-type heads of high and low frequency components are expressed as

$$\nu_1=39785.6+849.4(v'+1/2)-2.9(v'+1/2)^2-817.4(v''+1/2)+4.2(v''+1/2)^2\,,$$

$$\nu_2=37512.7+849.4(v'+1/2)-2.9(v'+1/2)^2-814.3(v''+1/2)+4.0(v''+1/2)^2\,.$$

Further, in the same region a new system ($F^2\Delta-X^2\Pi$) has been discovered both in absorption and in emission spectra of the arc. The observed constants of the upper state of this system are $\nu_0=38844\,\mathrm{cm}^{-1}$ and $\omega_0=588.5\,\mathrm{cm}^{-1}$.

Lakshman's ($C-X$) system has been confirmed on investigating emission spectra of arc and hollow cathode discharge from 2700 to 4400 A. Almost forty new heads are added to this system suggesting that the vibrational level of $v'=3$ in the higher component of the upper state is perturbed by a certain level. Also several bands are added to Lakshman's ($D-X$) system indicating that all v'' values of his vibrational scheme should be shifted by one quantum number upwards. The constants of this system have been revised as given below;

$$\nu=35049.8+499.9(v'+1/2)-3.0(v'+1/2)^2-817.3(v''+1/2)+4.2(v''+1/2)^2\,.$$

1. Introduction

The study on spectra of oxide molecules of Group V_b (Nitrogen Group) elements is well advanced except for heavier ones of the group. Concerning SbO molecule, Mukherji[1] was the first to publish a report on the analysis of its emission spectrum.

1) B. C. Mukherji: Z. Phys. **70** (1931) 552.

His light source was a carbon arc filled with metallic antimony and the bands that appeared in the region of 3374–5317 A were analysed to four singlet systems. Later in 1939 Sengupta[2] observed more bands using the same light source, and further, he analysed the many red shade bands that appeared in the region of 3245 A–6800 A to two doublet systems, ($^2\Sigma - ^2\Pi$) and ($^2\Pi - ^2\Pi$). These two systems have the same lower state, and he suggested this $^2\Pi$ state to be the ground state of separation 2272 cm^{-1}. In Sengupta's[3] report on "A New Ultra-Violet Band System of Antimony Monoxide" published in 1943, sixty heads in the region of 2452–2909 A were analysed to form a ($^2\Sigma - ^2\Pi$) system. However, because of no publication made of either the intensity estimation or the spectrograms of these systems, some doubt has been thrown upon his vibrational analyses.[4] On this account, re-investigation of the matter was undertaken in the present work. Very recently Lakshman[5] published an emission spectrogram in the region of 2850–4400 A, which was emitted from a heavy current discharge of hollow cathode type with nickel electrodes. He discovered two new systems, ($C\,^2\Delta - X\,^2\Pi$) and ($D\,^2\Sigma ? - X\,^2\Pi$). Further he made a rotational analysis of (0, 0) band of ($B\,^2\Sigma - X\,^2\Pi$) system and estimated the coupling constant of the lower state at 2276 cm^{-1}.[6]

All the above-mentioned reports are concerned with emission spectrum and no report on absorption has yet been published. It seemed necessary to take up the absorption spectrum of SbO, for the analysis of emission bands is difficult owing to overlapping of a number of bands appearing almost continuously from 2450 A to 8500 A. The author has photographed absorption and emission spectra of SbO and found new electronic states revising to fair extent the analyses thus far made.

Absorption spectrum appeared in the region from 2450 A to 2800 A. In comparison with the emission spectrum of this region, Sengupta's ultraviolet system[3] was investigated at first. Since the values of ω_e of the upper and lower states of this system are nearly equal and reversing of shade takes place even in one band causing extra heads to appear, construction of the spectrum is complicated. However, on the regularlity in the difference of these heads, analysis was made, and the result shows that vibrational constants of the upper state estimated this time are quite different from those obtained by Sengupta. Further, a new system, ($F(^2\Delta) - X\,^2\Pi$), and a partially analysed diffuse system, ($G - X\,^2\Pi$), were discovered in the same region.

2) A. K. Sengupta: Indian J. Phys. **13** (1939) 145.
3) A. K. Sengupta: Indian J. Phys. **17** (1943) 216.
4) R. W. B. Pearse and A. G. Gaydon: *The Identification of Molecular Spectra*, Chapman & Hall, London (1950).
5) S. V. J. Lakshman: Z. Phys. **158** (1960) 367.
6) S. V. J. Lakshman: Z. Phys. **158** (1960) 386.

All of these three systems have doublet seperation of approximately 2270 cm^{-1}, and Sengupta's suggestion as for the ground state was confirmed.

Lakshman's ($C\,^3\Delta - X\,^3\Pi$) system was verified by the investigation of the emission spectra of arc and hollow cathode discharge from 2700 A to 4400 A. Almost forty new heads are added to this system, and it is suggested that the vibrational level of $v'=3$ in the higher component of the upper state is perturbed by a certain level. As a result of examination of ($D-X$) system, several bands are added, which shows that one quantum number should be added to every v'' value of Lakshman's scheme.

2. Experimental Procedure and Appearance of Spectra

Arc is the most intense and easily tractable light source. The arc used by Mukherji and Sengupta emitted strong cyanogen bands, for melted antimony adsorbed carbon. But this can be avoided by using copper as a lower positive electrode instead of carbon. Input of about 10 A at D. C. 100 V through a resistance of 5–8 ohms gave rise to a white flame, almost 5 cm high in the air. The middle part of this flame emitted almost pure spectrum of SbO from 2450 A to 8500 A. All the bands displayed in the region longer than 2800 A appeared shading to red. In order to clarify the influence of impurities, boron-less carbon of high purity and antimony of six nine grade refined by the zone-melting method were used. However there was no difference in the appearance of the band spectrum when compared with that obtained on materials not so high in purity.

All the bands that appeared in the spectrum thus obtained were also observed in the emission of a high tension copper-copper arc run on supply of A. C. 7500 V with current regulated between 250 and 300 mA. A hole made on the top of the lower big copper rod electrode was filled with pure metallic antimony. Naturally this high tension arc emits no cyanogen band, however, oxyhydrogen bands and γ-system of nitric oxide disturbed the spectrum in the shorter wavelength region. This type of arc in oxygen at reduced pressure exhibits the band spectrum of low rotational temperature, although its intensity is much weaker than that of an ordinary arc.

A molybudenum hollow cathode of a discharge tube with D. C. 2000 V and 0.5–0.6 A input fed with pure Sb_2O_3 glows bluish purple displaying red shade bands, strong from 2780 A to 4500 A but weak in the longer wavelength region. This source of light is excellent in obtaining clearly ($B-X$), ($C-X$) and ($D-X$) systems designated by Lakshman.* When the discharge is well controlled, there appear neither atomic

*) Hereafter designations of elecronic states will follow Lakshman's. They are different from those used by Sengupta[2),3)] and those listed on page 567 in "Spectra of Diatomic Molecules" (1950) by G. Herzberg.

lines of molybudenum nor oxyhydrogen bands. But the atomic lines of antimony are more numerous and intense than in arc.

The spectra from 2300 A to 8900 A were photographed with various spectrographs. Glass spectrograph with three 60° prisms of 6 cm base was used for visible and near infra-red region. For ultra-violet region a Hilger E_1 quartz spectrograph was mainly used. Some spectra of arc photographed with a large concave grating spectrograph of almost 210,000 in theoretical resolving power and 665 cm in focal length served as a good reference.

The photographic materials employed were plates of Oriental Hyperpan, Fuji Neopan, Process Panchromatic and Process Hard and Kodak I-N, besides the films of Fuji SSS and Kodak 103-O U. V.. When arc or hollow cathode discharge was a light source, glass spectrograph needed merely from 30 seconds to a few minutes exposure, but high tension arc required considerably longer time. In the case of E_1 quartz spectrograph, exposure of several minutes was sufficient to take spectrum in the region of wavelength longer than 2800 A even with plates of Process Hard, however, it took about thirty minutes for the emission of arc in the shorter wavelength region. Even in this case the film of 103-O U. V. required only three minutes. With the grating spectrograph, suitable exposure on films of SSS or 103-O U. V. was 20 to 30 minutes.

The source for absorption spectrum was the discharge through flowing hydrogen purified by being passed through a palladium tube, and a flame from the arc mentioned above was the absorbing path. An E_1 quartz spectrograph was employed. It required the exposure of twenty minutes for Process Hard plate and two minutes for 103-O U.V. films. Since many bands were diffuse in the absorption spectrum, its photometric curve was traced in order to determine the position of heads.

Iron arc lines were photographed as reference standards on all of the plates and films used.

3. Analyses and Description of Bands; Discussion

When D. C. 100 V arc is a light source, four strong heads of (0, 0) sequence of cyanogen violet system appear line-like. Although there are several strong atomic lines of copper over the whole region, even the strongest head of CuO (6059.3 A) can be prevented from appearing on the photograph. When antimony of high purity is used in one of the electrodes, no atomic lines other than of antimony and copper mentioned above are emitted. Therefore, beside SbO, conceivable emitters of bands could be SbN and Sb_2. But there is no trace of the head of either of the two of which the particulars of the bands are already known. The emitter of the bands that appear seems to have no connection with carbon, for they are the same as those of high tension arc in which no carbon electrode is employed. In the case of hollow

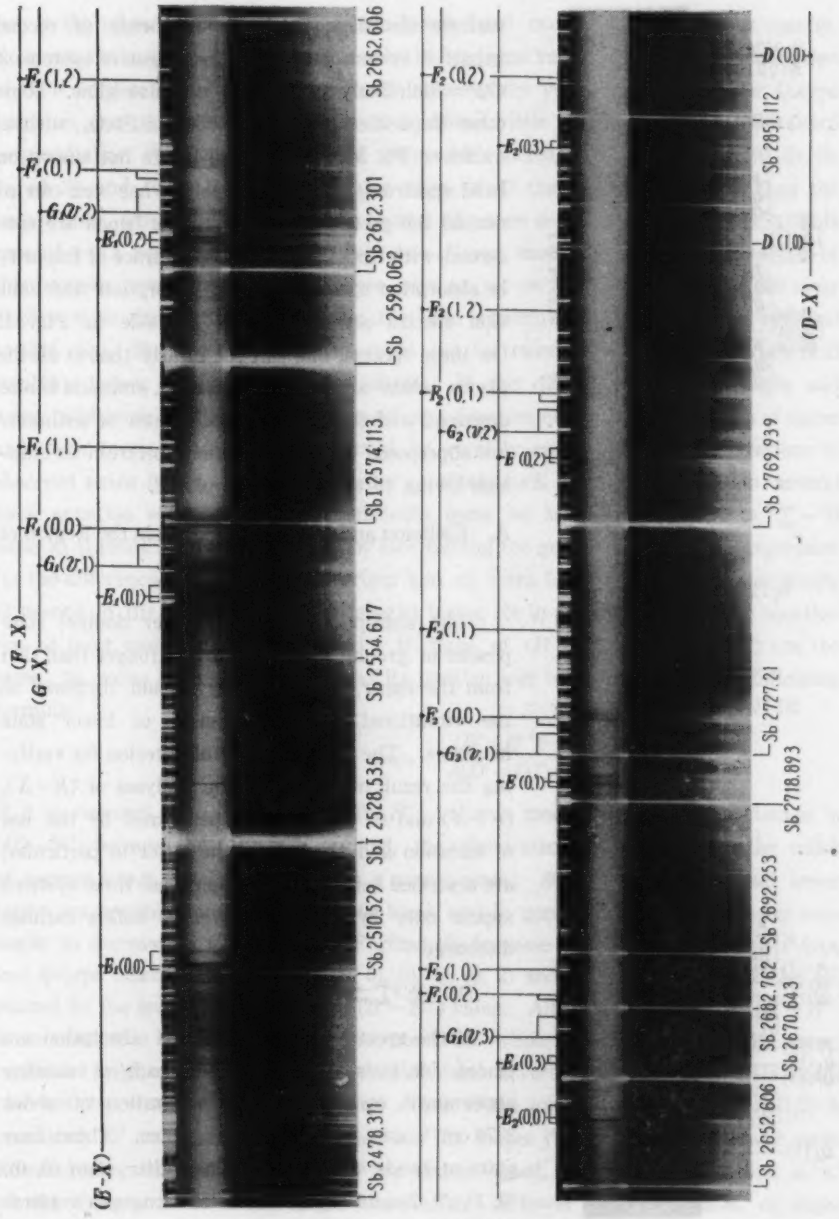

Fig. 1. Emission and absorption spectra.

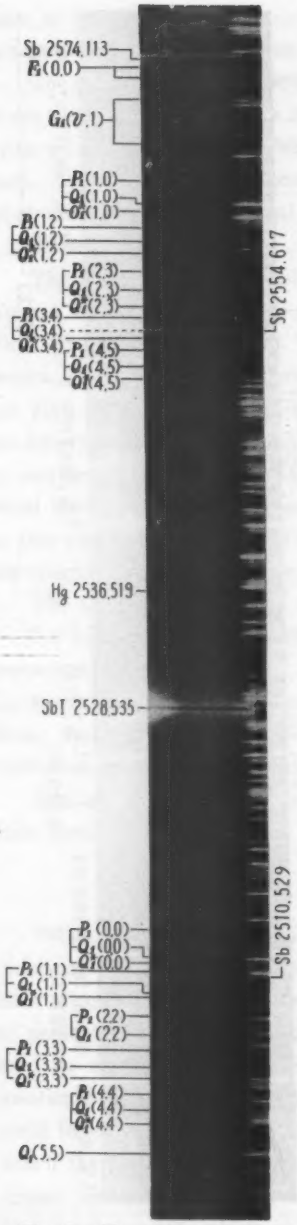

Fig. 2. Absorption spectrum.

cathode discharge there are no heads of second negative system of O_2^+ or first negative system of CO^+ which likely to appear in negative glow. Some other impurities possibly included in Sb_2O_3, such as oxides of Pb, Mg, Bi, As and P, are not shown on band spectrum. Therefore analysis has been carried out on the presumption that all the bands are concerned with SbO. There is also no trace of impurity in absorption spectrum. The absorption and emis sion spectra are shown side by side in Fig. 1. On these spectra, one can see clearly that at all the places, where absorption is apparent, emission is also apparent, and that some atomic lines of antimony are superposed on the absorption spectrum as emission owing to the method employed.

A. Emission and Absorption Spectra in the Region of 2450−2850 A

The absorption from the lower doublet component of ground state should be stronger than that from the upper, and intensity should decrease as the vibrational quantum number of lower state increases. The above is a useful criterion for verifying the result of analysis. The analyses of $(E-X)$, $(F-X)$ and $(G-X)$ systems performed by the use of emission and absorption, the latter in particular, are described below. In emission these three systems appear only by arcs and never by hollow cathode discharge.

(1) $(E\,^2\Sigma \rightleftarrows X\,^2\Pi)$ system

If the spectra of emission and absorption are placed side by side, four pairs of heads of simillar appearances, each pair with a separation of about 2270 cm^{-1}, can be seen at a glance. These four pairs of bands seem to be none other than (0, 0), (0, 1), (0, 2) and (0, 3) bands of Sengupta's ultraviolet system. Sengupta also reported (0, 4) bands,

but at the reported positions no violet shade head could be found in our spectra. However, the assignment of these four pairs of heads are verified by detailed examination of their appearance. Namely these bands are slightly violet-shaded and their Q-type branches are prominent, giving rise to a characteristic narrow "bands" with sharp long and short wavelength edges, and their width increases in the order of (0, 0), (0, 1), (0, 2) and (0, 3) band. The shorter edges of all the bands are weaker than the longer ones, which indicates that the shorter edges are so called "extra heads". This type of extra heads are found also in some P-type branches. Rotational analysis of this system was attempted, for there was as yet no published record on the clear display of so many extra heads in the transition between doublet terms as was revealed in this case. But the fine structure could not be traced on photographs of practical resolving power of not lower than 100,000. If the difference between origin and extra head were possible to be expressed as a function of rotational constants of upper and lower terms, these constants should be roughly estimable from the positions of observed extra heads. However, in order to obtain such a kind of expression, several cubic equation with complicated coefficients must be solved in the case of ${}^2\Sigma-{}^2\Pi$ (case a) transition. For the purpose of ascertaining the general tendency, an expression for the difference between the band origin and an extra head was obtained concerning Q branch in the transition between singlet terms, for in such a case the cubic equation can be most easily and simply solved. If signs of $(B'-B'')$ and $(D'-D'')$ are the same, an extra head should exist and its position can be expressed by the following formula:

$$\nu_{\text{extra head}} - \nu_{\text{origin}} = \frac{(B'-B'')^2}{4(D'-D'')} .$$

If it is assumed that a change in $(B'-B'')$ value is more effective than a change in $(D'-D'')$ because the former is squared, the above-mentioned increase in the width of narrow bands can be explained as a consequence: B_v values of upper and lower terms are possibly most close in (0, 0) band, and in general B_v'' values of lower state ought to decrease as v'' increases. Further the increase of difference between P-type and Q-type heads in the order of (0, 0), (0, 1), (0, 2) and (0, 3) band can also be explained by the increasing tendency of $(B'-B'')$ value. Although the value of $(B'-B'')$ is so small that many extra heads are observed, whole of a certain sequence seems to extend only to shorter wave length side, and reversal of shading of main heads can not be observed in any sequence. Thus if the expression $B_v=B_e-\alpha_e(v+1/2)$ is conceived, α_e' value of upper state can not be larger than α_e'' value of lower state. Remembering that α_e/B_e and $\omega_e x_e/\omega_e$ are nearly equal, we may presume that $\omega_e' x_e'$ of upper state can not be larger than $\omega_e'' x_e''$ of lower state, though ω_e' of upper state is a little larger than ω_e'' of lower state. In the analysis on ultra-violet system

Table 1. ($E^2\Sigma - X^2\Pi$) system.

λ A	ν cm^{-1}	Int. abs.	Int. emis.	shade	Assignment	remarks
2448.8	40824	1 d	1 d			narrow
50.0	804	1 d	1 d			wide
51.7	776	1 d	1 d		$Q_1(5, 4)$	narrow
53.8	741	1 d	1 d		$Q_1(4, 3)$	
55.2	718	1 d	1 d		$P_1(4, 3)$	
99.0	40004	1 d	1 d	v	$Q_1(5, 5)$	
2501.1	39970	1 d	1 d	r	$Q_1^*(4, 4)$	
01.8	959	2 d		v	$Q_1(4, 4)$	
03.1	938	3	2	v	$P_1(4, 4)$	
03.9	926	3	2 d	r	$Q_1^*(3, 3)$	
04.7	913	3		v	$Q_1(3, 3)$	
05.6	899	2	2	v	$P_1(3, 3)$	difference between P_1 & Q_1 is a little smaller than regularly expected.
06.5	884	1 d	1 d	r	$Q_1^*(2, 2)$	in a diffuse line
06.9	878	2	2	v	$Q_1(2, 2)$	in a diffuse line
07.8	864	2	1	v	?	
08.6	851	1	1	v	$P_1(2, 2)$	
09.0	845	5	3 d	r	$Q_1^*(1, 1)$	
09.4	838	5		v	$Q_1(1, 1)$	
09.8	832	2	2	v	?	
11.0	813	3	3	v	$P_1(1, 1)$	
11.3	808	7	2	r	$Q_1^*(0, 0)$	
11.7	802	10	3	v	$Q_1(0, 0)$	
13.5	773	4	3	v	$P_1(0, 0)$	
50.4	198	1 d	2 d		$Q_1^*(4, 5)$	diffuse iine
51.4	39182	1 d	2 d		$Q_1(4, 5)$	diffuse line
53.3	153	1 d	1 d		$P_1(4, 5)$?	differenee between P_1 & Q_1 is larger than regularly expected.
53.8	146	1 d	1 d	r	$Q_1^*(3, 4)$	
55.8	115	3	2	v	$P_1(3, 4)$	
56.8	100	1	1 d	r	$Q_1^*(2, 3)$	
57.8	084	2		v	$Q_1(2, 3)$	
58.8	069	2 d	1 d	v	$P_1(2, 3)$	
60.3	046	3	2 d	r	$Q_1^*(1, 2)$	
61.0	036	4		v	$Q_1(1, 2)$	
61.8	023	4	2	v	?	
62.3	016	1	1	v	$P_1(1, 2)$	
63.1	004	5	3 d	r	$Q_1^*(0, 1)$	
63.8	38993	8		v	$Q_1(0, 1)$	
64.6	981	5	3	v	?	
65.3	970	3	2	v	$P_1(0, 1)$	

λ A	ν cm⁻¹	Int. abs.	Int. emis.	shade	Assignment	remarks
2602.8	38409	1 d	1 d		$Q_{12}(2, 1)$	
03.2	403	2	2	*v*	?	
05.0	376	2	2	*r*	$Q_{12}^*(1, 0)$ & $Q_1^*(3, 5)$	
05.2	373	2 d	2 d	*v*	$Q_{12}(1, 0)$	in the shade of $Q_1(3, 5)$.
06.4	356	1	1	*v*	$Q_1(3, 5)$	
07.2	344	3	3	*r*	?	probably an extra head of a certain *R*-type branch.
08.1	331	3	3	*v*	$P_1(3, 5)$ & $P_{12}(1, 0)$	
09.4	312	1	2	*r*	$Q_1^*(2, 4)$	
10.2	300	2	2	*v*	$Q_1(2, 4)$	
11.4	282	2 d	1 d	*v*	$P_1(2, 4)$	
13.1	257	1 d		*r*	$Q_1^*(1, 3)$	
14.1	243	2 d	2 d		$Q_1(1, 3)$	line-like.
15.4	224	1		*v*	$P_1(1, 3)$	
16.5	208	5	4	*r*	$Q_1^*(0, 2)$	
17.6	192	6	5	*v*	$Q_1(0, 2)$	
18.0	186	3		*r*	$P_1^*(0, 2)$	emission is masked by Cu I 2618.366.
18.9	173	4	4	*v*	$P_1(0, 2)$	
47.5	37760	1 d		*r*	$Q_{12}^*(5, 5)$	
48.8	742	1 d	2 d	*v*	$Q_{12}(5, 5)$	
54.0	668	2	2	*v*	$P_{12}(4, 4)$	
55.5	647	3 d	3 d	*v*	$Q_{12}(3, 3)$	diffuse line.
56.7	629	2 d	2 d	*v*	$P_{12}(3, 3)$	difference between Q_{12} & P_{12} is a little smaller than regularly expected value.
58.0	611	1 d	2 d	*v*	$Q_{12}(2, 2)$	
59.8	586	2 d	2 d	*v*	$P_{12}(2, 2)$	
61.1	567	2 d	3 d		$Q_{12}(1, 1)$	diffuse line.
62.0	555	2 d	2 d	*r*	$P_{12}^*(1, 1)$	
63.1	539	2 d	2 d	*v*	$P_{12}(1, 1)$	
63.4	535	4	2	*r*	$Q_{12}^*(0, 0)$	
63.7	531	5	5	*v*	$Q_{12}(0, 0)$	
64.7	517	2 d	2 d	*v*	?	
65.2	509	2	2	*r*	$P_{12}^*(0, 0)$	
66.0	498	2	3	*v*	$P_{12}(0, 0)$	
68.8	459	1 d	1 d		$Q_1(1, 4)$	
72.9	401	3	3	*v*	$Q_1(0, 3)$	
74.2	383	2 d	3 d		$P_1(0, 3)$	diffuse line.
2707.8	36919		1 d	*v*	$Q_{12}(4, 5)$	
10.5	883		1 d	*r*	$Q_{12}^*(3, 4)$	
11.7	866		1 d	*v*	$Q_{12}(3, 4)$	
12.4	857	2 d	3	*r*		probably an extra head of (0, 1) band; close double head on the spectrum of grating.
13.3	845		3	*v*	$P_{12}(3, 4)$	

Table 1. (Continued).

λ A	ν cm^{-1}	Int. abs.	Int. emis.	shade	Assignment	remarks
2714.6	37827		2	r	Q_{12}*(2, 3)	
15.2	819	1	2	v	Q_{12}(2, 3)	
16.6	36800	1 d	2 d	v	P_{12}(2, 3)	difference between Q_{12} & P_{12} is a little smaller than expected.
17.9	782	1 d	1 d		Q_{12}*(1, 2)	
20.4	748	2	3	v	P_{12}(1, 2)	
21.3	736	2	5	r	Q_{12}*(0, 1)	
22.2	724	4	7	v	Q_{12}(0, 1)	
23.2	711	3	5	r	P_{12}*(0, 1)	
24.1	699	3	5	v	P_{12}(0, 1)	
68.7	107		2 d	r	Q_{12}*(3, 5)	
71.5	071		3	v	P_{12}(3, 5)	
73.3	048	1	3	r	Q_{12}*(2, 4)	overlapped by some another extra head.
74.1	037		2	v	Q_{12}(2, 4)	
78.7	35977	1	3	v	Q_{12}(1, 3)	
79.7	964		2	r	P_{12}*(1, 3)	
80.5	954		2	v	P_{12}(1, 3)	
81.2	945	2	5	r	Q_{12}*(0, 2)	
82.5	928	3	7	v	Q_{12}(0, 2)	
84.1	908	2	6	v	P_{12}(0, 2)	
2840.5	35195		0.5 d		Q_{12}(1, 4)	
41.9	177		0.5 d		P_{12}(1, 4)	
42.4	171		2	r	Q_{12}*(0, 3)	
43.2	161		2 d	v	?	
44.7	143		3 d	v	Q_{12}(0, 3)	
46.1	125		3	v	P_{12}(0, 3)	

worked out by Sengupta, the constants were derived accurately from data of sixty heads, and Q-heads of high and low frequency components were given by the following formulae respectivly;

$$\nu_1 = 39767.7 + 879.90(v' + 1/2) - 5.90(v' + 1/2)^2 - 817.5(v'' + 1/2) + 5.20(v'' + 1/2)^2 ,$$

$$\nu_2 = 37495.7 + 880.0(v' + 1/2) - 5.80(v' + 1/2)^2 - 817.0(v'' + 1/2) + 5.20(v'' + 1/2)^2 .$$

Sengupta's results are of little avail for detailed comparison with the present data, for he did not refer to the appearance of heads. Nevertheless, even if the error in the author's measurement is fully taken into account, almost one third of the number of heads in Sengupta's analysis are not found in the author's spectra, or in other words, Sengupta's analysis could not be verified. Therefore, for the explanation of the present data, an analysis of the obtained photographs was made anew on the basis

of the regularity mentioned above, and its results are listed in Table I. Possibly the listed wave numbers have errors of 5–6 cm^{-1} or more on account of the difficulties of precise measurement, because fair number of bands are weak and appear as though diffuse lines. In the column of intensity, "d" means diffuse. In the column of shade, "v" and "r" mean that the measured values are for long wavelengh side and short wavelength side respectively of the bands. For narrow bands of indeterminable shade, measurements were made at their middle. There are listed also some prominent heads which are not assigned but seem to have some connection with this system. For instance, the violet shade head at 2564.6 A that appeared sharply in both emission and absorption spectra is likely to be assigned to $P_1(0, 1)$ head, but such an assignment makes the difference between $P_1(0, 1)$ and $Q_1(0, 1)$ too small. There is a possibility of this being a head in a sequence following the $G(v, 0)$ band, which will be described later. But there are similar heads lying also between Q- and P-type heads of some other bands. Heads of this kind appear at 2507.8, 2509.8 and 2561.8 A. A red shade head at 2712.4 A is a very close double head only barely resolved on the spectrum taken with a large grating spectrograph. This head appears also in absorption with the intensity next to the heads of (0, 1) band, while the other bands of this sequence are very weak in absorption. Therefore this may be an extra head in a certain branch of (0, 1) band, which is usually to have no head. The close double head structure can possibly be explained by the rotational isotope effect of $Sb^{121}O$ and $Sb^{123}O$, since this head should be formed at quite a high J value. A red shade head at 2773.3 A, conspicuous in emission, can be faintly observed also in absorption, Though this head appears at a position suitably assignable to an extra head of $Q_{12}(2, 4)$, its intensity seems to indicate that a certain extra head of (0, 2) bands is overlapping. There is one more red shade head at 2607.2 A which can be regarded as of the same kind. However, they are away from their origins at long distances of 133, 120 and 152 cm^{-1} respectively in the order given above, which leaves a problem yet to be solved.

Table 2 is a Deslandres Table of the newly analysed ($E \rightleftarrows X$) system. Merely Q-type heads are listed for simplicity. Small numbers in parentheses indicate intensities of emission and absorption, the first for emission and the second for absorption. In this table, bands lie along the diagonal illustrating the characteristic more clearly than in Sengupta's analysis. As regards the separation between vibrational levels in the upper state, $\Delta G_{1/2}$ and $\Delta G_{3/2}$ are nearly equal in value, and the level $v'=2$ is most likely shifted upwards by perturbation of some level, this shift being estimated at 3–4 cm^{-1}. When it comes to the change of intensity in a sequence, it is strange that all the bands that are related to $v'=2$ level are weaker in intensity than those that are related to $v'=3$ level in the upper state, but this will be explained if we assume

Table 2. Deslandres Table of

v' \ v''	0		1		2
0	(3) (10) 39802 [0] (2271) (5) (5) 37531 [+0.5]	809 807	(3 d) (8) 38993 [0] (2269) (7) (4) 36724 [−0.2]	801 796	(5) (6) 38192 [−0.4] (2264) (7) (3) 35928 [+2.1]
	—— 842		845 843		844 ——
1	(2 d)(2 d) 38373 [−1.1]	806	(3 d) (5) 39838 [+1.4] (2271) (3d)(2d) 37567 [−0.8]	802 ——	(2d)(4) 39036 [−0.4] masked by Sb 2718.893
			—— 842		842 ——
2			(1d)(1d) 38409 [+3.4]	798	(2d)(2) 39878 [+4.2] (2267) (2d)(1d) 37611 [+3.7]
3					
4					
5					

* These values are too small because Q_{12} head of (0, 3) band is of a wavelenth shorter should be the partner of Q_1 (0, 3) head.

The small numbers in ( ) are estimated intensities; the first for emission, and the

the $v'=2$ level as being perturbed. With the vibrational constants of upper and lower states, corrected for the effect of this perturbation, Q-type heads of high and low frequency components are expressed as

(E–X) system.

	3		4		5
791	(3) (3) 37401 [+0.8]				
	(2258)				
785*	(3) 35143 [+7.4]				
	842				
	834*				
793	(2) (2) 38243 [−0.8]	784	(1d) (1d) 37459 [−0.1]		
	(2266)		(2264)		
——	(3) (1) 35977 [−2.2]	782	(0.5) 35195 [−1.9]		
	841		841		
	842		842		
794	(1d) (2) 39084 [+2.4]	784	(2) (2) 38300 [+2.2]		
	(2265)		(2263)		
792	(2) (1) 36819 [+2.0]	782	(2) 36037 [+2.3]		
	829		——		
	828		829		
	(2d) (3) 39913 [−0.6]	——	masked by		(1) (1) 38356 [+1.6]
	(2266)		Sb 2554.617		masked by
	(3d)(3d) 37647 [−2.0]	781	(1d)(1d) 36866 [−0.7]		Sb 2769.939
	828		——		826
	——		——		——
	(1d)(1d) 40741 [+1.2]	782	(1d)(2d) 39959 [+3.0]	777	(2d)(1d) 39182 [+1.4]
			masked by		(2263)
			Sb 2652.606		(1d)(0.5d) 36919 [+0.4]
			817		822
			——		823
			(1d)(1d) 40776 [−0.4]	772	(1d)(1d) 40004 [+3.0]
					(2262)
					(2d)(1d) 37742 [+3.0]

than expected. However the appearance of this band clearly shows that only this head second for absorption. The values in [ ] are ($\nu_{obs.}-\nu_{cal.}$).

$$\nu_1=39785.6+849.4(v'+1/2)-2.9(v'+1/2)^2-817.4(v''+1/2)+4.2(v''+1/2)^2,$$
$$\nu_2=37512.7+849.4(v'+1/2)-2.9(v'+1/2)^2-814.3(v''+1/2)+4.0(v''+1/2)^2.$$

The differences between observed and calculated wave numbers obtained from the

above formulae are listed on Table 2 in brackets. The low frequency component of (0, 3) band is situated where the wavelength is somewhat shorter than what the proposition of regularity expects, which put Deslandres Table partially out of order. However, the appearance of this head clearly shows that this head should be the very partner to $Q_1(0, 3)$ head of the doublet and can be nothing else. The vibrational constants of the lower state derived above are almost equal to those obtained from $(A-X)$, $(B-X)$ and $(C-X)$ systems. Therefore these four systems are presumed to

Table 3.

$(F(^2\Delta) \rightarrow X^2\Pi)$ system, red shade.

v'' / v'	0		1		2
0	(1) (3) 2572.8 λ (3)(10) 2573.6 38856.5 ν 38844.5	808.4	(1) (2) 2627.3 (4) (5) 28.3 38050.6 036.1	800.4	(1) (1) 2683.8 (3) (2) 84.8 37249.6 235.7
	(2) (1) 2732.5 λ (5) (3) 33.4 36585.7 ν 573.7	804.8	(2) (1) 2793.8 (5) (2) 94.9 35783.0 768.9	798.2	(1) 2857.3 (4) (1) 58.7 34987.8 970.7
	591.4		586.3 589.3		586.0 589.6
1	λ ν		(2) (1) 2588.4 38622.4	800.7	(1) (1) 2642.4 (1) (1) 43.2 37833.1 821.7
	(1) (1) 2689.0 λ (1) (1) 89.9 37177.5 ν 165.1	806.9	(2) 2749.6 36358.2	797.9	(2) 2811.3 35560.3

Numbers in ( ) are estimated intensities; the first for emission and the second for absorption.

have the lower state in common. The fact that the absorption from the lower state was evidenced, verifies that the state is the ground state of SbO suggested by Sengupta.

(2) $(F(^3\Delta)\rightleftarrows X\,^3\Pi)$ system

The result of analysis is listed on Table 3. All bands of this system are shaded to long wavelength side. The heads of (0, 0), (0, 1) and (0, 2) bands are situated opposite to violet shade heads of (0, 1), (0, 2) and (0, 3) bands of $(E-X)$ system respectively. It is remarkable in this system that, in absorption, high frequency component is stronger than the low one and the intensity rapidly decreases as v'' increases. In emission, low frequency component is much stronger than high frequency one. Most of the bands shows a strong Q-type head resembling a diffuse line. This feature is plainly shown in absorption of (0, 0) band of high frequency component but is absent in emission presumably because of self absorption. In all the bands no rotational structure is found in the proximity of head, but at the region a little distance away from the head the difference between rotational lines increases rapidly, and there are a few bands for which rotational analysis on spectrograms of high resolution seems possible. A weak head is attaching to each Q-type head with a seperation of about $12-17\,cm^{-1}$. Therefore upper state may be considered a $^2\Sigma$ or a regular $^2\Delta$ with close doublet seperation, since the difference between each pair of heads is about $2270\,cm^{-1}$ or a little smaller. All bands that are related to $v'=1$ are very weak in comparison with those related to $v'=0$, and no band related to $v'=2$ is found. Thus accurate values of ω_e and ν_e can not be determined and rough estimation gave $\omega_0=588.5\,cm^{-1}$ and $\nu_{00}=38845\,cm^{-1}$. The lower state has obviously the constants almost equal to those of $X\,^3\Pi$.

(3) Diffuse system; $(G\rightleftarrows X\,^3\Pi)$ system

There lie two diffuse bands, strong and weak, between two opposing heads in each of (0, 1) band of $(E-X)$ system and (0, 0) band of $(F-X)$ system, (0, 2) band of $(E-X)$ system and (0, 1) band of $(F-X)$ system, and (0, 3) band of $(E-X)$ system and (0, 2) band of $(F-X)$ system. Although diffuse, their longer wavelength edges seem a little sharper and almost all the bands appear shading to violet. With these edges as heads, and strong and weak heads as pairs, Table 4 was prepared. The stronger head of (v, x) band of this system appears on the long wavelength side, 64–65 cm^{-1} from Q-type head of $(0, x)$ band of $(E-X)$ system. Therefore these diffuse heads may be considered to have some connection with $(E-X)$ system, yet, even a trace of heads of such kind, which should belong to (0, 0) band, is not found. Since the difference between these strong and weak heads amounts to 45–50 cm^{-1}, in order to regard them as Q- and P- type heads, values of rotational constants of the upper and lower terms should not be very different. Thus ω_e values of upper and

Table 4.
Diffuse system; ($G \rightleftarrows X$) system.

v'' / v'	1		2		3
	2566.7–68.1 V		2620.3–21.8 V		2677.1–77.5 V
λ	70.3–71.4 V		24.9–25.6 V		80.0–80.7 d
	(3) (7) 38949–928	798	(4) (3) 38152–130	793	(3) (2) 37343–337
ν	(2) (2) 894–878		(2) (1) 085–075		(2) (1) 302–293
v	2271		2270		
	2726.2–27.2 V*		2786.4–87.8 V		
λ	30.0–31.0 V		90.7–91.3 V		
	(5) (2) 36670–657	797	(4) (1) 35878–860		
ν	(3) (1) 619–606		(2) 823–815		

* Continued to Sb 2727.21.

Nnmbers in ( ) are estimated intensities; the first for emission and the second for absorption.

lower states should be nearly equal and these diffuse bands may be considered overlapped by many bands of a certain sequence. In such a case, it is strange to find no trace of (0, 0) sequence which should appear the strongest of all the sequences of the system. Even on spectrograms of high resolution, no fine structure is revealed. Yet, in all probability, this system is related to the ground state of SbO molecule, for we are convinced of a doublet separation of approximately 2270 cm^{-1} being there.

B. Emission Spectrum in the Region of (2700–4400 A)

Analyses of emission spectra are carried out by using both spectra of arc and hollow cathode discharge. The shortest wavelength region of the latter spectrum is shown in Fig. 3.

(1) ($C^2\Delta - X^2\Pi$) system

By analysis of ($C-X$) system, Lakshman gave a reasonable Deslandres table with fourty-three heads including high frequency components of vibrational levels up to $v''=5$ in the lower state and $v'=12$ in the upper state, and low frequency components of those up to $v''=3$ and $v'=11$. Most part of these bands is found in our spectra within the experimental error of 5 cm^{-1}. However, there remain many other similar bands yet unanalysed. And among them the bands which can be suitably expressed

Table 5.
$(C-X)$ system; red shade.

λ	ν	Int.	Assignment	$\nu_{obs.}-\nu_{cal.}$	remarks
3017.3	33132.6	3	$C_1(8, 1)$	+2.6	
3139.7	31841.0	4	$C_1(4, 0)$	−0.9	revised L's value.
3148.2	31755.0	3	$C_1(10,4)$	−4.1	
3194.5	31294.8	4	$C_1(6, 2)$	+2.4	overlapped by the longer head of close double head of $C_1(3, 0)$.
3212.0	31124.3	1	$C_2(9, 2)$	−2.3	
3249.4	30766.1	1	$C_1(5, 2)$	+2.1	
3250.8	30752.8	3	$C_1(8, 3)$	+1.1	orverlapped by the shorter head of close double head of $C_1(2, 0)$.
3254.5	30717.9	2	$C_1(11,6)$	+5.0	
3306.9	30231.1	2	$C_1(4, 2)$	+2.5	
3318.0	30130.0	3	$C_2(4, 0)$	+3.6	
3321.0	30102.8	3	$C_2(7, 2)$	+0.9	revised L's value.
3335.5	29971.9	2	$C_1(5, 3)$	+0.6	
3337.0	29958.5	2	$C_1(11,7)$	+1.4	
3374.4	29626.4	6d	$C_1(0, 0)$	−3.5	revised L's value.
3380.1	29576.5	4d	$C_2(3, 0)$	−8.0	$v'=3$ level is shifted downwards about 5 cm^{-1}.
			$C_2(6, 2)$	−3.2	
3393.1	29463.1	2	$C_1(7, 5)$	0	
			$C_1(10,7)$	−0.8	
3475.1	28767.9	2	$C_2(3, 1)$	−6.7	$v'=3$ level is shifted downwards about 5 cm^{-1}.
3504.2	28529.1	2	$C_2(7, 4)$	+0.9	
3568.3	28016.6	5	$C_2(9, 6)$	+0.6	overlapped by $C_1(0, 2)$.
3586.5	27874.4	5	$C_1(4, 5)$	−3.6	probably overlapped by a head of $(B-X)$ system which is not yet reported.
3645.5	27423.3	2	$C_2(2, 2)$	−2.1	
			$C_1(6, 7)$	+2.4	
3656.8	27338.6	4	$C_1(3, 5)$	+3.1	overlapped by $B_1(3, 1)$.
3678.8	27175.1	1d	$C_2(3, 3)$	−7.2	$v'=3$ level is shifted downwards about 5 cm^{-1}.
3702.2	27003.3	4	$C_1(1, 4)$	−0.6	
3711.2	26937.8	4	$C_2(4, 4)$	−4.2	
3720.4	26871.2	1	$C_2(1, 2)$	+0.8	masked by SbII 3722.793 in hollow cathode spectrum, though clear in arc.
3731.8	26789.1	4	$C_1(2, 5)$	+3.0	overlapped by $B_1(2, 1)$.
3744.0	26701.8	2	$C_2(5, 5)$	−2.5	
3781.1	26439.8	5	$C_1(0, 4)$	−0.5	clear head in spite of being in the shade of $B_1(0, 0)$.
3811.3	26230.3	4	$C_1(1, 5)$	+0.7	overlapped by $B_1(1, 1)$.
3820.4	26167.9	2	$C_2(4, 5)$	−1.1	
3833.4	26079.1	2d	$C_2(1, 3)$	+1.1	
3872.1	25818.5	1	$C_1(3, 7)$	+3.8	
3895.3	25664.7	5	$C_1(0, 5)$	−1.3	overlapped by $B_1(0, 1)$.
3926.8	25458.8	4	$C_1(1, 6)$	−5.7	
4015.7	24895.2	1	$C_1(0, 6)$	+4.2	
4076.6	24523.3	5	$C_2(1, 5)$	−0.4	overlapped by $B_2(2, 1)$.
4208.1	23757.0	3	$C_2(1, 6)$	−2.9	probably overlapped by a certain head of some other system.
4242.2	23566.1	3	$C_2(2, 7)$	+5.8	
4309.3	23199.1	2	$C_2(0, 6)$	+0.7	

Table 6.
Intensity distribution of $(C-X)$ system.
(I) $(C\,^2\Delta_{3/2}-X\,^2\Pi_{1/2})$ component

v'' / v'	0	1	2	3	4	5	6	7
0	6r	5	5	6	**5**	**(5)**	**1**	
1	4	4	4		**4**	**(4)**	**4**	
2	4	2	3	4	3	**(4)**		
3	4		2	2		**(4)**		**1**
4	4r		**2**			**(3)**		
5	4	**3**	**1**	**2**		2		
6	3	2	**(4)**					**(2)**
7	2	3		3		**2**		
8	2	**3**		**(3)**				
9		2	2					
10					**3**	3		**(2)**
11					**(3)**		**2**	**2**

(2) $(C\,^2\Delta_{3/2}-X\,^2\Pi_{3/2})$ component

v'' / v'	0	1	2	3	4	5	6	7
0	5	5					**2**	
1	4	2	**1**	**2**		**(5)**	**(3)**	
2	3		**(2)**					**3**
3	**(3)**	**2**		**1**				
4	**3**				**4**	**2**		
5	4					**2**		
6	3		**(3)**					
7	(4)		(3)r		**2**			
8	3	2		3				
9	(3)		**1**				**(5)**	
10								

r Lakshman's value revised. ( ) overlapped head. Newly added heads are given in Gothic.

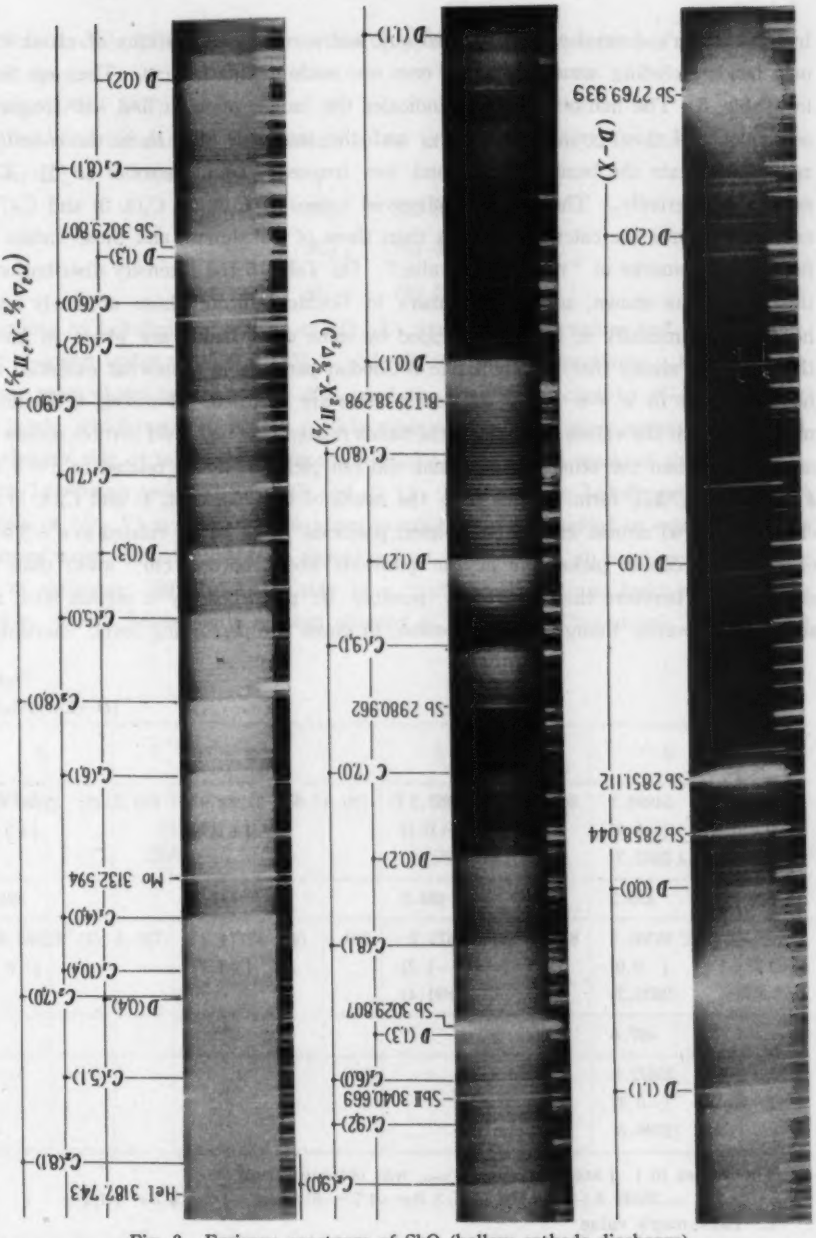

Fig. 3. Emisson spectrum of SbO (hollow cathode discharge).

by Lakshman's formulae were picked out, and a reasonable addition of about forty new heads including some overlapped ones was made to this system. They are listed in Table 5. The marks C_1 and C_2 indicates the bands of high and low frequency components of this system respectively, and the marks B_1 and B_2 in the column of remarks indicate the bands of high and low frequency components of ($B^2\sum - X^2\Pi$) system respectively. The author's observed values of $C_1(0, 0)$, $C_1(4, 0)$ and $C_2(7, 2)$ are much nearer the calculated values than those of Lakshman, and these values are listed with remarks of "revised L's value". On Table 6 the intensity distribution of this system are shown, and the numbers in Gothic indicate those of newly added heads. The intensity of bands overlapped by some other bands are given in parentheses. This shows that the right side of Condon parabola is somewhat extended and bands related to $v''=6$ and 7 of lower state are revealed. However, it should be mentioned that the values concerning the bands related to $v''=7$ level involve somewhat more errors than the others. Lakshman did not pick out bands related to $v'=3$ and 4 levels of $C^2\Delta_{5/2}$ term. This time the heads of $C_2(4, 1)$, $C_2(4, 4)$ and $C_2(4, 5)$ are clearly observed almost at their calculated positions. The bands related to $v'=3$ level of $^2\Delta_{5/2}$ term can be picked out at the positions about several cm^{-1} lower than the calculated. Therefore this level may possibly be perturbed by a certain level and shifted downwards, though it is impossible to guess the perturbing level. According

Table
($D \rightarrow X$) system,

v' \ v''	0		1		2		3
0	(3) 34890.1 [−0.9] (λ 2865.3)	807.9	(4) 34082.2 L [+0.1]	799.3	(5) 33282.9 L [+1.3]	793.3	(5) 32489.6 L [+0.1]
	495.2		*493.0		491.3		494.2
1	(2) 35385.3 [0.0] (2825.2)	810.1	(4) 34575.2 [−1.2] (2891.4)	801.0	(4) 33774.2 L [−1.7]	790.4	(3) 32983.8 L [0.0]
	487.6						
2	(2) 35872.9 [−0.3] (2786.8)						

The values in [ ] are ($\nu_{obs.}-\nu_{cal.}$); $\nu_{cal.}$ was obtained from
$\nu=35049.8+499.9(v'+1/2)-3.0(v'+1/2)^2-817.3(v''+1/2)+4.2(v''+1/2)^2$.

L. Lakshman's value

* These values are much higher than the calculated, however, they are clear new heads

to Table 6, vibrational levels are verified up to $v'=11$ of $^2\Delta_{3/2}$ term and $v'=9$ of $^2\Delta_{5/2}$ in our spectra.

(2) ($D^2\Pi - X^2\Pi$) system

The lower states of all the systems so far investigated are $X^2\Pi$, and its observe $\Delta G_{v''+1/2}$ are as follows:

$\Delta G_{1/2}$ 805–811

$\Delta G_{3/2}$ 797–802

$\Delta G_{5/2}$ 789–794.

According to Lakshman's scheme of ($D-X$) system, $\Delta G_{1/2}$ values and $\Delta G_{3/2}$ values, both of lower states are 799.3, 803.7 and 793.3, 790.4 respectively. However, the former seem closer to $\Delta G_{3/2}$ than $\Delta G_{1/2}$ and the latter seem close to $\Delta G_{5/2}$. Actually, two heads, which seem to belong to this system, are found, each appearing on short wavelength side of and approximately 810 cm^{-1} away from each of the two heads, which Lakshman assigned to (0, 0) and (0, 1). Therefore in Lakshman's vibrational scheme of ($D-X$) system, one quantum number should be added to every v'' value of lower state. What Lakshman picked out as a head of (1, 0) band seems an atomic line of antimony, 2891.214 A, for this is a fairly weak line and looks as if forming a close double heads with a head situated at 2891.4 A. This atomic line does not

7.

red shade.

	4		5		6
782.9	(4) 31706.7 [+0.9] (3153.0)	763.5	(2) 30943.2* [+12.7] (3230.8)		
					(3) 30670.7* [+12.8] (3259.5)

and listed for reference.

appear in the spectrum of arc, and all other bands belonging to this system seem to be single, at least in the spectrum taken with a prism spectrograph. Therefore if the head at 2891.4 A is assigned to the head of (1, 1) band, the above-mentioned value, 803.7 cm^{-1}, should change to 801.0, which seems better as a $\Delta G_{3/2}$ value. With these corrections made and several new heads added, Table 7 was prepared. There is one and only one band that relates to $v'=2$ level of the upper state. Judged from its appearance, fine structure and position, we are sure of this to be the head of (2, 0) band of this system. There remain many unclassified heads of similar type, but they can neither be listed on Deslandres Table so as to extend this system nor clearly be analysed as another doublet component. According to Lakshman's report, the upper state of this system is marked with $^2\Sigma$?. If it is a $^2\Sigma$ state, another component of this system should appear with a separation of about 2270 cm^{-1}. But no partner of this component can be found at the expected position. Further, all heads are single as already mentioned. Hence, it is reasonable to consider the upper state to be $^2\Pi$ rather than $^2\Sigma$.

(3) Other bands

If fairly strong red shade heads left unanalysed are picked out in the vicinity of $(D-X)$ system, a sheme as follows can be obtained.

Table 8.

(3)	34668.7	792.9	(4) 33875.8	779.4	(2 d) 33096.4
			671.9		
			(4) 34547.7		
			666.9		
			(4) 35214.6		

Numbers in parenthses indicate intensity.

A scheme having similar differences can also be obtained with red shade heads around 3400 A as follows.

Table 9.

(3) 29074.1	789.6	(3) 28284.5
673.1		670.9
(2) 29747.2	791.8	(2) 28955.4

Some conspicuous heads are so far tentatively dealt with, however, there still remain many heads, clear and fairly strong. Further study is needed for their analyses.

C. Discussion

The existence of seven electronic states, X, A, B, C, D, E and F of SbO molecule was ascertained and their vibrational constants were obtained by the analyses so far

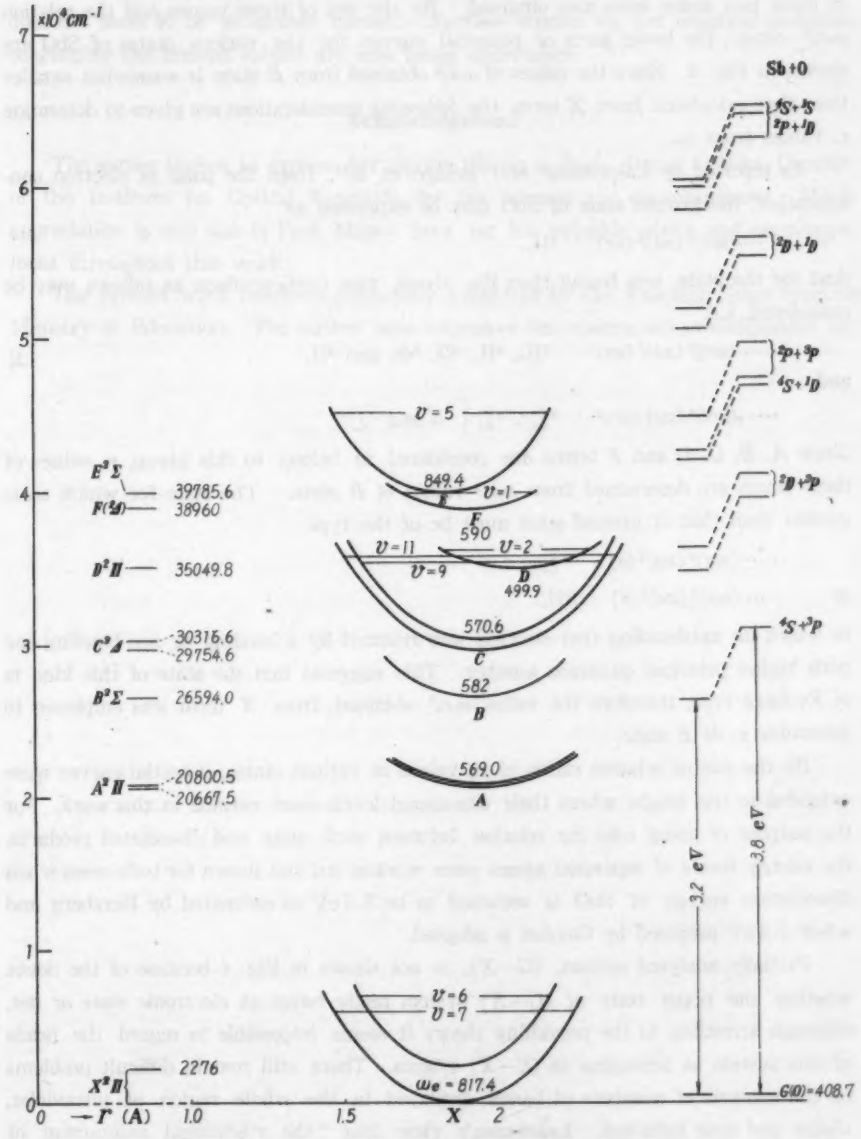

Fig. 4. Partial potential curves of SbO.

made. From the rotational analysis of (0, 0) band of ($B^2\Sigma \rightarrow X^2\Pi$) system, r_e values of these two states were also obtained. By the use of these values and the relation $\omega_e r_e^2$=const., the lower parts of potential curves for the various states of SbO are shown in Fig. 4. Since the values of $\omega_e r_e^2$ obtained from B state is somewhat smaller than that calculated from X term, the following considerations are given to determine r_e values from ω_e.

As reported by Lakshman[6] and Bridge et al[7], from the point of electron configuration, the ground state of SbO may be expressed as

$$\cdots\cdots(w\pi)^4(x\sigma)^2(v\pi) \qquad {}^2\Pi_r.$$

And for the state, less bound than the above, two configurations as follows may be considered, i. e.

$$\cdots\cdots(w\pi)^3(x\sigma)^2(v\pi)^2 \qquad {}^2\Pi_r,\ {}^2\Pi_i,\ {}^2\Pi,\ {}^2\Phi_i \text{ and } {}^4\Pi_i$$

and

$$\cdots\cdots(w\pi)^4(x\sigma)(v\pi)^2 \qquad {}^2\Sigma^+,\ {}^2\Sigma^-,\ {}^2\Delta \text{ and } {}^4\Sigma^-.$$

Since A, B, C, D and F terms are considered to belong to this group, r_e values of these states are determined from $\omega_e r_e^2$ values of B state. The state for which ω_e is greater than that of ground state must be of the type

$$\cdots\cdots(w\pi)^4(x\sigma)^2(\sigma) \qquad {}^2\Sigma$$

or $$\cdots\cdots(w\pi)^4(x\sigma)^2(\pi) \qquad {}^2\Pi,$$

in which an antibonding ($v\pi$) electron was replaced by a bonding or non-bonding one with higher principal quantum number. This suggests that the state of this kind is of Rydberg type, therefore the value $\omega_e r_e^2$ obtained from X term was employed to determine r_e of E state.

By the use of relative ratios of ω_e values of various states, potential curves were extended to the height where their vibrational levels were verified in this work. For the purpose of going into the relation between each state and dissociated products, the energy levels of separated atoms were worked out and shown for both cases when dissociation energy of SbO is assumed to be 3.8 eV as estimated by Herzberg and when 3.2 eV proposed by Gaydon is adopted.

Partially analysed system, ($G-X$), is not shown in Fig. 4 because of the doubt whether the upper state of ($G-X$) system really forms an electronic state or not, although according to the prevailing theory it seems impossible to regard the heads of this system as belonging to ($E-X$) system. There still remain difficult problems on the analysis of numbers of bands displayed in the whole region of ultraviolet, visible and near infra-red. Lakshman's view that "the vibrational assignment of

7) N. K. Bridge and H. G. Howell: Proc. Phys. Soc. A. **67**, (1954) 44.

bands of $(A-X)$ and $(B-X)$ systems in agreement with those proposed by Sengupta" does not seem to be altogether correct. Further studies on yet unsolved problems concerning the present subject are now being undertaken.

Acknowledgement

The author wishes to express her sincere thanks to Prof. Haruo Ootuka, Director of the Institute for Optical Research, for his interest and encouragement. Much appreciation is also due to Prof. Masao Seya for his valuable advice and encouragement throughout this work.

The present work has been financially supported by the Research Grant from the Ministry of Education. The author also expresses her sincere acknowledgement for it.

Ionization of Alkali Elements in Flame

Ryohei ISHIDA

Government Chemical Industrial Research Institute, Sibuya-ku, Tokyo

(Received, September, 14, 1960)

Abstract

From flow-rates of fuels and atomized volumes of sample solutions, partial pressures of alkali elements in oxy-hydrogen flame are calculated, and from these values, degrees of ionization of alkali elements are obtained by the equation of Saha.

On the assumption that the spectral line intensity is proportional to the concentration of neutral atoms, relative intensities of spectral lines and theoretical working curves are obtained. These calculated values are close to the experimental values.

1. Introduction

Fundamental of Saha's ionization formula is explained by Gaydon[1]. For the formula to be exact in numerical application, contribution of upper electronic states of atoms to the specific heat, that is the electronic partition function, should be made known, but for the present purpose, it is sufficient to regard the atoms, ionized atoms and electrons as constituting the ideal gas, an electron being assumed to possess the molecular weight of 1/1845.

The equilibrium constant K is given by the ratio of the partial pressures

$$K=[A^+][e]/[A]=\frac{x^2}{1-x^2}\cdot P$$

in which it is assumed that, $[A^+]=[e]$, and x is then the ionized fraction of the initial amount A, and P is the sum of partial pressures in atomospheres.

The Saha's equation then takes the numerical form

$$\log K=\log\left(\frac{x^2}{1-x^2}\right)=-U/4.573\,T+\frac{5}{2}\log T-6.49+\log\left(\frac{g_{A^+}\cdot g_e}{g_A}\right).$$

Here, U is the ionization potential of A atoms, expressed as a positive quantity in calories/mole; $U=23053\times I$, where I is the ionization potential in electron volts; T is the temperature in $^\circ K$; g_{A^+}, g_A and g_e are the statistical weights of the ionized atom,

1) A. G. Gaydon and H. G. Wolfhard; *Flames Their Their Structure, Radiation and Temperature* (1953) p. 282.

the neutral atom and the electron respectively.

For the electron, because of its spin, $g=2$. For the atom and ionized atom $g=2J+1$, where J is the quantum number for total angular momentum of the electron in ground state (for a multiplet as the ground state, g will be the sum of the values of $2J+1$ for the components). For alkali metals, with $^2S_{1/2}$ as the ground state, $g_A=2$, and for the ionized alkali metales, with $^1S_0$ as the ground state, $g_{A^+}=1$, so the final term becomes $\log 1=0$.

In the case of oxy-hydrogen flame, which was used in this experiment, $T=2400°K$ was obtained[2]. This reduces Saha's equation to

$$\log \frac{x^2}{1-x^2}\cdot P=-23053\times I/4.573\times 2400+5/2\ \log 2400-6.49$$
$$=-2.1\times I+1.96.$$

The ionization potential is 5.37 eV for lithium, 5.12 eV for sodium, 4.32 eV for potassium, 4.16 eV for rubidium and 3.87 eV for cesium. With these numerical values, the above equation becomes

for Li, $\log\frac{x^2}{1-x^2}\cdot P=-11.27+1.96=-9.31=\overline{10}.69=\log(4.9\times10^{-10})$,
for Na, 〃 $=\log(1.005\times10^{-9})$,
for K, 〃 $=\log(7.76\times10^{-8})$,
for Rb, 〃 $=\log(1.70\times10^{-7})$,
for Cs, 〃 $=\log(6.76\times10^{-7})$.

2. Calculation of flow-rate of oxy-hydrogen

Measurement and calculation were made on oxy-hydrogen flames, Beckman-type atomizer-burner being used in the measurement. Oxygen and hydrogen were, one at a time, let through the burner at the same rates as used in the flame experiments in this work and their rates were read on a flow-meter and on a gas-meter at the same time.

1) Calibration of the flow-meter

The flow-meter was of U-tube type filled with liquid paraffin. Out of several size capillary tube, the one that suited most was used at the center position A in Fig. 1.

Air from a valve-controlled compressed air reservoir was let through the flow-meter and the gas-meter connected in series as shown in Fig. 1. By calibration against the gas-meter, the flow-meter readings—the level differences between B and C in Fig.

2) R. Ishida; Chem. Soc. Japan, Pure Chem. Sec. **79** (1956) 238 (in Japanese).

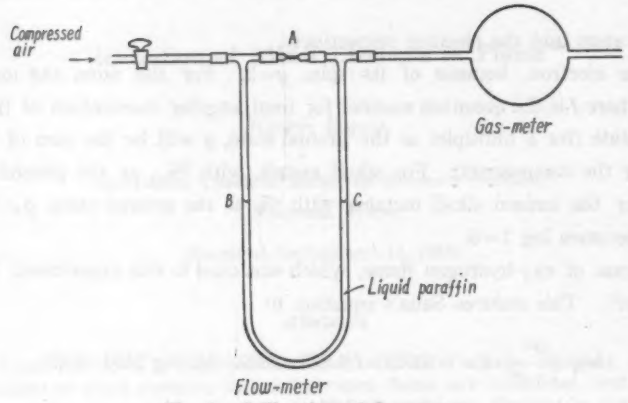

Fig. 1. Calibration of flow-meter.

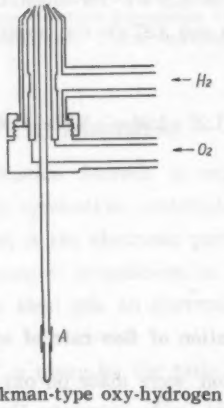

Fig. 2. Beckman-type oxy-hydrogen burner.

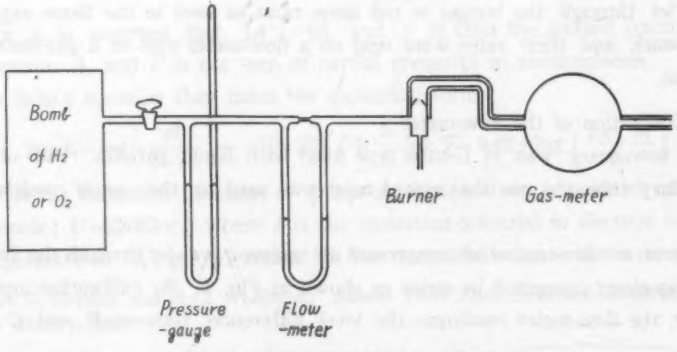

Fig. 3. Measurement of gas flow.

1—of 0~18 cm corresponded to 0~4 l/sec flow-rates by the latter.

2) Measurement of flow-rate under burning condition

Sectional view of Beckman-type atomizer-burner is shown in Fig. 2 in which the lower end A of the capillary, from which sample solutions are let in, is shown closed to keep the tube free from air.

The measurement was made with the arrangement shown in Fig. 3. Pressure of oxygen or hydrogen gas from the valve-controlled reservoir is read on a U-tube pressure gauge; the gas is let flow through the flow-meter to the atomizer-burner. At the exit of the burner, the gas pressure becomes 1 atm., and the flow-rate is read on the gasmeter. Measurement is repeated 2~3 times and the mean of the readings is used for calculation. Results obtained on oxygen are given in Table 1 and those on hydrogen in Table 2. The reduction of flow-meter readings taken under pressure to flow-rates at normal pressure is performed as follows.

Table 1. Calculated and observed values of gas flow (oxygen).

No. of Experiment	Pressure			Flow-meter reading (mean value) cm	Rate of gas flow	
	lb/in	kg/cm	atm.		Calculated from flow-meter reading l/min	Gasmeter reading l/min
1	24.6	1.79	1.73	5.70	3.44	5.54
2	25.3	1.84	1.78	6.00	3.64	3.72
3	26.0	1.89	1.83	6.23	3.83	3.89
4	27.0	1.96	1.90	6.60	4.10	4.01
5	27.9	2.03	1.96	6.76	4.29	4.19
6	28.9	2.10	2.03	7.08	4.56	4.37

Table 2. Calculated and observed values of gas flow (Hydrogen).

No. of Experiment	Pressure			Flow-meter reading (mean value)	Rate of gas flow	
	lb/in	kg/cm	atm.		Calculated from flow-meter reading l/min	Gasmeter reading l/min
1	14.5	1.052	1.018	4.35	6.97	8.03
2	14.8	1.072	1.037	10.25	11.04	12.50
3	15.0	1.093	1.057	16.20	14.73	15.74

If t is the duration of flow and d the density of the gas, we have

$$t_2/t_1 = \sqrt{d_2/d_1}$$

and if v is the volume of flow in time t and M the molecular weight of the gas

$$v_1/v_2 = t_2/t_1, \quad d_2/d_1 = M_2/M_1.$$

Hence

$$v_1/v_2 = \sqrt{d_2/d_1} = \sqrt{M_2/M_1}.$$

Since

$$\sqrt{M_{air}} = \sqrt{28.9} = 5.38,$$
$$\sqrt{M_{O_2}} = \sqrt{32} = 5.65,$$
$$\sqrt{M_{H_2}} = \sqrt{2} = 1.414,$$

from the above relation of $v_1 = v_2\sqrt{M_2/M_1}$, we have for the gas volumes

$$O_2 = \text{Air} \times 5.38/5.65 = \text{Air} \times 0.95$$
$$H_2 = \text{Air} \times 5.38/1.414 = \text{Air} \times 3.81$$

These values, when multiplied by the pressure read on the pressure gauge, give the flow-rates of the gases. For example, for oxygen, flow-meter reading $\times 0.95 \times$ pressure gauge reading gives its flow-rate.

3. Calculation of the partial pressure

From the above experiment, the pressures and the flow-rates of oxygen and hydrogen under operating condition become

Pressure	Flow-rate
for oxygen at 2 atm = 2.067 kg/cm² = 28.4 lb/in²	4.1 l/min,
for hydrogen at 1.037 atm = 1.072 kg/cm² = 14.8 lb/in	12.5 l/min.

Under these conditions and when the atomizer-burner atomized a solution into the flame, flow rate of the solution that passed the position A in Fig. 3 was 1.0 ml/min. This value is approximately 1 g/min which is, when vapourized, $22.41 \times 1/18 = 1.244$ liter per minute.

Accordingly, the total flow-rate of the gases that constitute the flame is obtained as follows.

The reaction between oxygen and hydrogen in flaming is $2H_2 + O_2 = 2H_2O$. Hence the flow-rate of oxygen required for combusion with hydrogen of the flow-rate of 12.5 l/min is 6.25 l/min in which 4.3 l/min—the first oxygen—was from the reservoir,

therefore, 6.25−4.3=1.95 l/min—the second oxygen—was from the surronnding air for combusion. This makes the flow-rate of nitrogen that mixed into the flame as 1.95 l/min×4=7.80 l/min.

The flow-rate of gas mixture during the combustion is calculated as follows. 8.6 l/min of H_2O vapour which is produced in inner cone of the flame by the reaction between the first oxygen and a part of the hydrogen, 3.9 l/min of unreacted hydrogen, and 7.80 l/min of nitrogen that came with 1.95 l/min of the second oxygen, a total of 22.25 l/min is the sum of flow-rates of all the gases that go through the outer cone. At the end of the reaction, 12.5 l/min of H_2O vapour, which corresponds to the rate of consumed hydrogen and 7.8 l/min of nitrogen, a total of 20.3 l/min is produced.

The second oxygen and the accompanied nitrogen enter between inner cone and the top of outer cone of the flame, therefore the flow-rate of gas mixture through the outer cone which is used for flame spcctrophotometry is considered to be approximately equal to the above flow-rate of 20.3 l/min of the gas mixture at the end of reaction. This flow is at room temperature of 25°C, hence it is necessary to reduce the flow-rate to that at 0°C normal state, which becomes 20.3 l/min× 273/(273+25)=18.6 l/min, and by adding to this the flow-rate 1.244 l/min of the vapour, we obtain 19.8 l/min for the final total flow-rate of flame gas reduced at 0°C normal state.

On the other hand, if for example, the concentration of alkali elements in solution is 100 mg/l, the rate of atomization will be 100 mg/l×1 ml/min=0.1 mg/min. The atomic weights of Li, Na, K, Rb and Cs being 6.94, 23.0, 39.1, 85.5 and 132.9 respectively, flow-rates of these elements as gases in normal state will then be

Li : $22.4\,l\times0.0001\,g/min/6.94\,g=3.23\times10^{-1}\,l/min$,
Na : $22.4\,l\times0.0001\,g/min/23\,g=0.974\times10^{-4}\,l/min$,
K : $22.4\,l\times0.0001\,g/min/39.1\,g=0.573\times10^{-4}\,l/min$,
Rb : $22.4\,l\times0.0001\,g/min/85.5\,g=0.262\times10^{-4}\,l/min$,
Cs : $22.4\,l\times0.0001\,g/mln/132.9\,g=0.1685\times10^{-4}\,l/min$.

Partial vapour pressure of these elements in the flame will therefore be by Dalton's rule

$P_{Li}=3.23\times10^{-4}\div19.8=1.63\times10^{-5}$ atm,
$P_{Na}=4.92\times10^{-6}$ atm,
$P_{K}=2.89\times10^{-6}$ atm,
$P_{Rb}=1.32\times10^{-6}$ atm,
$P_{Cs}=8.51\times10^{-6}$ atm.

From these values, partial pressures of the elements in the flame when their concent-

rations in solution are other than 100 mg/l can be found. The partial pressures when concentrations of 100, 80, 60, 40, and 20 mg/l are used are given in Table 3.

4. Calculations of ion concentration and percentage of neutral atoms in the flame

By the use of the values given in Table 3 and from the values of $x^2/(1-x^2)P$ obtained in Section 1, values of ionized fractions, x, of the alkali elements were calculated and are given in Tahle 4.

Since the values in Table 4 are the fractions of A^+ ions, the assumption $[A^+]=[e]$ made in Section 1 means that the numbers of ions and electrons are the same. The sum of partial pressures at atmospheric pressure becomes $([A-A^+]+[A^+]+[e])P=([A]+[e])P$ which becomes eventually $\{[A]\times(1+x_1)\}P$ because the products of the values in Table 3 and those in Tabie 4 are the values of $[A^+]$. Here, x_1 represents the values given in Table 4. If we use $\{[A]+(1+x_1)\}P$ instead of the values given

Table 3. Partial pressures of alkali elements in the flame.

Element \ Concentration*	100	80	60	40	20
Li	1.63×10^{-5}	1.30×10^{-5}	0.978×10^{-5}	0.652×10^{-5}	0.326×10^{-5}
Na	4.92×10^{-6}	3.94×10^{-6}	2.95×10^{-6}	1.97×10^{-6}	0.987×10^{-6}
K	2.89×10^{-6}	2.31×10^{-6}	1.73×10^{-6}	1.16×10^{-6}	0.578×10^{-6}
Rb	1.32×10^{-5}	1.056×10^{-6}	0.792×10^{-6}	0.528×10^{-6}	0.264×10^{-6}
Cs	8.51×10^{-7}	6.81×10^{-7}	5.11×10^{-7}	3.40×10^{-7}	1.70×10^{-7}

Table 4. Fraction of the ionized atoms (x).

Element \ Concentration*	100	80	60	40	20
Li	5.48×10^{-3}	6.15×10^{-3}	7.08×10^{-3}	8.68×10^{-3}	$1,23\times10^{-2}$
Na	1.43×10^{-2}	1.60×10^{-2}	1.84×10^{-2}	2.25×10^{-0}	3.19×10^{-0}
K	1.62×10^{-1}	1.80×10^{-1}	2.07×10^{-1}	2.52×10^{-1}	3.45×10^{-1}
Rb	0.339	0.373	0.421	0.495	0.626
Cs	0.666	0.707	0.756	0.816	0.894

* Concentration in mg/l of element in water solution for atomization.

Table 5. Most probable values of the fractions of ionized atoms.

Element \ Concentration*	100	80	60	40	20
Li	5.47×10^{-3}	6.12×10^{-3}	7.05×10^{-3}	8.63×10^{-3}	1.21×10^{-2}
Na	1.42×10^{-2}	1.58×10^{-2}	1.83×10^{-2}	2.23×10^{-2}	3.15×10^{-2}
K	1.50×10^{-1}	1.67×10^{-1}	1.90×10^{-1}	2.27×10^{-1}	3.06×10^{-1}
Rb	0.300	0.328	0.368	0.429	0.543
Cs	0.580	0.616	0.665	0.731	0.827

Table 6. Percentage of the neutral atoms in flame.

Element \ Concentration*	100	80	60	40	20
Li	99.45	99.39	99.29	99.14	98.78
Na	98.58	98.42	98.17	97.77	96.85
K	85.0	83.3	81.0	77.3	69.4
Rb	70.0	67.2	63.2	57.1	45.7
Cs	42.0	38.4	33.5	26.9	17.3

in Table 3, the values of the fractions become different from what are given in Table 4. Representing these new values by x_2, we obtain another set of values represented by x_3 if we use $\{[A]+(1+x_3)\}P$ instead of $\{[A]+(1+x_1)\}P$. After numbers of repetition of calculation, we see that $x_5=x_6=x_7=x_8\cdots$. Hence the values represented by x_5 are taken as the most probable values of the fractions which are given in Table 5.

From the values of fractions of ionized atoms, percentages of neutral atoms were obtained as given in Table 6.

Percentages of neutral atoms, when water solutions of the elements of concentrations other than those given in Table 6 are used, are given in Table 7 and Table 8. The degree of ionization is notably high by low concentrations but is very low by high concentrations.

* See page 140.

Table 7. Percentage of the neutral atoms in flame.

Element \ Concentration*	100	80	60	40	20
Li	98.28	98.08	97.79	97.29	96.19
Na	95.58	95.08	94.33	93.12	90.40
K	59.9	56.4	51.8	45.2	33.2
Rb	33.9	30.2	25.7	19.9	12.0
Cs	10.2	8.5	6.6	4.6	2.4

Table 8. Percentage of the neutral atoms in flame.

Element \ Concentration*	1000	800	600	400	200
Li	99.83	99.81	99.78	99.73	99.61
Na	99.55	99.50	99.42	99.28	98.99
K	94.92	94.37	93.53	92.15	89.03
Rb	89.3	88.1	86.35	83.56	77.6
Cs	75.5	73.1	69.6	64.3	53.8

5. Problem of the working curve in flame-spectrophotometry

General appearance of working curve in oxy-hydrogen flame-spectrophotometry is as shown in Fig. 4. For preparing the working curve, sensibility of the meter for measuring spectral line intensity of the element in hand was so adjusted that 100 mg/l concentration of the element in its water solution gave full scale reading of 100 when the solution was atomized in the flame.

The working curves for elements of small atomic weights are convex toward the intensity axis while those of larger atomic weight have a tendency of becoming concave as are seen in Fig. 4. The reason why the working curves for lithium and sodium, the lighter elements, are convex toward the intensity axis is being explained by the self-reversal of resonance lines, which weakens the line intensity as the concentration is raised. On the other hand, the tendency that potassium, rubidium and cesium, the heavier elements, have is considered attributable to their low ionizing

* See Page 140.

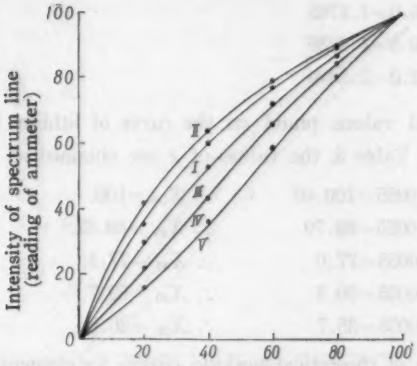

Fig. 4. Experimental working curves of Bockman-type oxy-hydrogen flame. I Lithium 6707.85 Å II Sodium 5889.9, 5895.9 Å III Potassium 7644.9, 7699.0 Å IV Rubidium 7800.3, 7947.6 Å V Cesium 8521.1, 8943.5 Å

potential to their being easily ionized at low concentrations in the flame, leaving only a small number of neutral atoms and thereby weakening the line intensity at low concentrations.

For the confirmation of the above, working curves are theoretically derived from the ionization data obtained in the preceding section. At first, it is assumed that the self-absorption is the same for all the elements concerned, for their spectral lines belong to the same spectral terms of $^2S_{1/2}-^2P_{3/2}$ and $^2S_{1/2}-^2P_{1/2}$ and that the electron configurations in outer orbit are the same. On this assumption, derivation of a theoretical standard curve was made on lithium, the element that undergoes the least ionization. Let X_{100}, X_{80}, X_{60}, X_{40}, and X_{20} be the spectral line intensities at respective concentrations read on the theoretical standard working curve that is yet to be determined. The line intensity obtained with 100 mg/l lithium solution in oxy-hydrogen flame at 2400°K should due to neutral lithium atoms which is, according to Table 6, 99.45% of the whole. Therefore, since this 99.45% was made to give the full scale reading of 100 in preparing the experimental working curve, values found on the experimental curve will be 100/99.45 times larger than what would be given by the theoretical working curve. Let this conversion ratio be F. From Table 6, F for each of the concerned elements becomes

F (Li) : 100/99.45=1.0055
F (Na) : 100/98.58=1.0144

F (K) : 100/85.0=1.1765
F (Rb) : 100/70.0=1.4286
F (Cs) : 100/42.0=2.3810

From experimental values found on the curve of lithium in Fig. 4 and by the use of values given in Table 6, the values of x are obtained as follows;

$X_{100}\times 99.45\times 1.0055=100.00$ $\therefore X_{100}=100$,
$X_{80}\times 99.39\times 1.0055=89.79$ $\therefore X_{80}=89.82$.
$X_{60}\times 99.29\times 1.0055=77.0$ $\therefore X_{60}=77.1$,
$X_{40}\times 99.14\times 1.0055=59.5$ $\therefore X_{40}=59.7$,
$X_{20}\times 98.78\times 1.0055=35.7$ $\therefore X_{20}=36.0$.

For the calculation of theoretical working curves for elements other than lithium from the above theoretical values of intensity and the use of percentages, a, of neutral atoms of the concerned elements, the equation (theoretical value)=(value of the standard working curve)$\times a\times F$ will serve. The results of calculation are given in Table 9 in which the numerical values in parentheses are the experimental values of Fig. 4. The values of Table 9 give the theoretical working curve as shown in Fig. 5. These calculated curves are similar in charactristics to those shown in Fig. 4 which were obtained by observation.

6. Discussion

In this work, the self-reversal is assumed to occur to the same extent in intensity

Table 9. Values of the calculated working curve.

Element \ Concentration*	100	80	60	40	20
Li	100	89.75	77.0	59.5	35.7
Na	100	89.66 (90.00)	76.8 (79.0)	59.2 (63.2)	35.3 (41.5)
K	100	88.02 (86.8)	73.47 (72.2)	54.3 (52.2)	29.3 (29.7)
Rb	100	86.22 (84.5)	69.61 (66.0)	48.7 (43.3)	23.5 (21.9)
Cs	100	82.11 (80.7)	61.5 (57.8)	38.2 (35.8)	14.8 (15.7)

* See page 140.

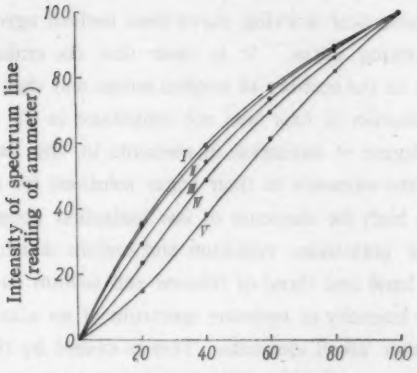

Fig. 5. Calculated working curves for the use of Beckman-type oxy-hydrogen flame
I Lithium 6707.85 Å, II Sodium 5889.8, 5895.9 Å
III Potassium 7644.9, 7699.0 Å, IV Rubridium 7800.3, 7947.6 Å V Cesium 8521.1, 8943.5 Å,

to all the resonance lines of the alkali elements.

In addition, there are negative ions produced in the flame. Among them, it is O^- that will play an important role; this ion is believed to have the electron affinity of about 2.20 eV. If ionizable metal vapours such as of alkali elements are present in the flame, $[e]=[A^+]-[0^-]$ may be assumend, and we treat the equilibrium between O^- and O as of a single ionization with ionization potential of 2.2 eV. On the assumption that the statistical weight term is log 3, then at a partial pressure of 10^{-4} of oxygen atoms at 2000°K, only about 6% of free electrons would be found attached to oxygen atoms. At 3000°K, if 3% of oxygen atoms are present, about one third of the electrons would be attached to them[4]. The production of negative ions will increase the total number of ions only a little and reduce the concentration of free electrons also only a little. In the present work, all these effects of the negative ions are ignored in the calculation.

Lastly, the calculation of partial pressures in the flame was based on the volume ratio of participating gases after combustion.

The three assumptions mentioned above are involved in the results obtained in the present experiment. Nevertheless, when the degree of ionization of elements in the flame is calculated by Saha's formula and from it the intensities of spectral lines

4) See ref. 1 p. 284.

are obtained on the assumption that the intensity is proportional to the number of neutral atoms, the theoretical working curve thus derived agrees approximately with the experimental working curve. It is clear that the emission of atomic spectral lines is in proportion to the number of neutral atoms and that the creation of excitation state by recombination of ions does not contribute to the emission.

As regards the degree of ionization of elements in the flame, it is high when the concentration of the elements in their water solutions for atomization is low and vice versa; it is also high for elements of low ionization potential and vice versa as seen in the cases of potassium, rubidium and cesium which have a low ionization potential on the one hand and those of lithium and sodium on the other.

Generally the line intenslty of emission spectrum of an alkali element is enhanced by the presence of other alkali elements. This is caused by the change in the state of ionization equilibrium and this effect is inferred to be much smaller on lithium and sodium than on potassium, rubidium and cesium.

The reversal of the order of working curves for lithium and sodium in Fig. 4 is explained mostly by the fact that, among alkali elements, lithium combines with OH forming LiOH much more than the others[5] and partly by the difference in photometrical arrangement: For the determination of line intensity for sodium, a multiplier phototube 1 P-28 was used while for the rest a red colour sensitive phototube was used.

7. Conclusion

From flow-rates of fuels and atomized volumes of alkali sample solutions, partial pressures of alkali elements in oxy-hydrogen flame are calculated, from which the degrees of ionization of the elements in the flame are obtained by the equation of Saha.

Analysis of working curves proved that the spectral line intensity of alkali elements is in proportion to the number of neutral atoms present in the flame. Rise of excitation state by recombination of ions does not contribute to the line intensity.

The above resuls explain the characteristics of working curves in flame spectrophotometry. Enhancing of line intensity when two or more alkali elements are present in the flame is also explained by the the change in the state of ionization equilibrium. This effect is inferred to be very large on potassium, rubidium and cesium.

5) H. Smith and T. M. Sugden: Proc. Roy. Soc. London **219** (1953) 204.
C. G. James and T. M. Sugden: Nature, Lord., **171** (1953) 428.

CONTENTS

Preparation of Uniform Layer of Sodium Salicylate
.....F. MASUDA and M. SEYA 99

Absorption Coefficients of Trans-dichlorethylene in the Vacuum Ultraviolet .....K. GOTO 104

Emission and Absorption Spectra of SbO in the Ultraviolet.....M. SHIMAUCHI 109

Ionization of Alkali Elements in Flame.....R. ISHIDA 134

9572